

Genome-wide analysis of spatiotemporal gene expression patterns during early embryogenesis in rice

Jun-Ichi Itoh^{1,*}, Yutaka Sato², Yutaka Sato³, Ken-Ichiro Hibara¹, Sae Shimizu-Sato³, Hiromi Kobayashi¹, Hinako Takehisa², Karen A. Sanguinet⁴, Nobukazu Namiki⁵ and Yoshiaki Nagamura²

ABSTRACT

Embryogenesis in rice is different from that of most dicotyledonous plants in that it shows a non-stereotypic cell division pattern, formation of dorsal-ventral polarity, and endogenous initiation of the radicle. To reveal the transcriptional features associated with developmental events during rice early embryogenesis, we used microarray analysis coupled with laser microdissection to obtain both spatial and temporal transcription profiles. Our results allowed us to determine spatial expression foci for each expressed gene in the globular embryo, which revealed the importance of phytohormone-related genes and a suite of transcription factors to early embryogenesis. Our analysis showed the polarized expression of a small number of genes along the apical-basal and dorsal-ventral axes in the globular embryo, which tended to fluctuate in later developmental stages. We also analyzed gene expression patterns in the early globular embryo and how this relates to expression in embryonic organs at later stages. We confirmed the accuracy of the expression patterns found by microarray analysis of embryo subdomains using *in situ* hybridization. Our study identified homologous genes from *Arabidopsis thaliana* with known functions in embryogenesis in addition to unique and uncharacterized genes that show polarized expression patterns during embryogenesis. The results of this study are presented in a database to provide a framework for spatiotemporal gene expression during rice embryogenesis, to serve as a resource for future functional analysis of genes, and as a basis for comparative studies of plant embryogenesis.

KEY WORDS: Embryogenesis, Rice, Transcriptome, Gene expression, Microarray, Microdissection

INTRODUCTION

In higher plants, embryogenesis is a process that establishes the body plan required for early vegetative growth after germination. Early embryogenesis includes crucial developmental events for organizing plant architecture; namely, establishment of embryo polarity, pattern formation, and the differentiation of distinct cell types, tissues and organs. Although these determination processes are common among plant species, there are differences in the

patterns of cell division and determination processes (Natesh and Rau, 1984; Steeves and Sussex, 1989; West and Harada, 1993). The genetic and molecular mechanisms underlying developmental processes during embryogenesis have been investigated in the model eudicot *Arabidopsis thaliana*. One of the advantages of *Arabidopsis* for such studies is its morphologically simple structure. In addition, *Arabidopsis* embryos undergo an invariant cell division pattern to generate diverse cell types and tissues, allowing cell lineages to be traced (Jenik et al., 2007). Embryonic studies of *Arabidopsis* also benefit from the abundance of genetic and genomic resources. Forward and reverse genetics studies increase our understanding of the molecular basis of embryo polarity and pattern formation, as well as cell type, tissue and organ differentiation mechanisms (Breuninger et al., 2008; Smith and Long, 2010; Ueda et al., 2011; Lau et al., 2012). Furthermore, genome-wide expression analyses using microarray and RNA-seq have been used for embryonic studies to estimate the number of genes expressed and predict the gene families associated with developmental and metabolic processes during embryogenesis (Nodine and Bartel, 2010; Xue et al., 2011; Palovaara et al., 2013). Transcriptome analyses combined with laser-capture microdissection during *Arabidopsis* embryogenesis revealed global expression features in different parts of embryos and within embryos of different developmental stages (Casson et al., 2005; Spencer et al., 2007; Le et al., 2010; Belmonte et al., 2013).

Although it is important to determine whether the genetic programs governing embryo development during plant embryogenesis are evolutionarily conserved among various plant species, molecular genetic work has mostly been conducted in *Arabidopsis* and is not as well understood in other species. Rice embryogenesis is a good candidate for comparative genetic studies, although the rice embryo has a morphologically complex structure and the early embryo is deeply embedded in ovary tissues (Itoh et al., 2005b). Rice embryogenesis exhibits biologically novel features not observed in *Arabidopsis*. First, because the embryo does not show stereotypic cell division patterns, embryonic cell types and tissues cannot typically be traced back to the early cell lineage. Second, the rice embryo shows an evident dorsal-ventral polarity whereby the shoot initiates on the ventral side and the scutellum forms dorsal side. Third, a radicle is endogenously differentiated in the center of the early embryo. Fourth, complex embryo-endosperm interactions affect embryo development and growth throughout embryogenesis (Itoh et al., 2005b; Nagasawa et al., 2013; Zhou et al., 2013). Thus, elucidation of the molecular mechanisms governing embryo development in rice will provide novel insights into embryogenesis of grasses and contribute to the diversity of embryonic studies in higher plants.

Functional analyses of genes involved in rice embryogenesis have been mainly performed using forward genetics approaches. One of the reasons why reverse genetics have not been applied to

¹Department of Agricultural and Environmental Biology, Graduate School of Agricultural and Life Sciences, University of Tokyo, Tokyo 113-8657, Japan.

²Genome Resource Unit, Agrogenomics Research Center, National Institute of Agrobiological Sciences, Kannondai 2-1-2, Tsukuba, Ibaraki 305-8602, Japan.

³Department of Bioresource Sciences, Graduate School of Bioagricultural Sciences, Nagoya University, Nagoya 464-8601, Japan. ⁴Department of Crop and Soil Sciences, Washington State University, Pullman, WA 99164, USA. ⁵Genome Informatics Department, Mitsubishi Space Software Co., Ltd., Takezono 1-6-1, Tsukuba, Ibaraki 305-0032, Japan.

*Author for correspondence (ajunito@mail.ecc.u-tokyo.ac.jp)

embryonic studies in rice is the limited number of knockout lines publicly available. In addition, knockdown techniques such as RNAi or artificial miRNA are not successful because transgenic plants are typically generated from calli in rice and genes regulating embryo development and fertility are usually not silenced in regenerated plants. However, recent advances in genome editing techniques have improved the feasibility of the study of embryonic lethal null alleles. These techniques allow observation of null phenotypes of essential genes required for embryogenesis in rice. In particular, it has been shown that the clustered regularly-interspaced short palindromic repeats (CRISPR)/Cas9 system is able to efficiently knockout multiple paralogous genes in rice for subsequent characterization (Endo et al., 2015). Thus, our understanding of the genetic regulation of embryo development will improve using genome editing-based reverse genetics.

For future functional analyses of grass embryogenesis, genome-wide expression profiling is necessary. Although expression profiling of various embryonic tissues and stages has been reported in rice and maize (Jiao et al., 2009; Takacs et al., 2012; Xu et al., 2012; Xue et al., 2012; Lu et al., 2013; Chen et al., 2014), predicting the spatial expression pattern and dynamics of gene expression during early embryogenesis remains difficult.

In this study, we performed transcriptome profiling of rice embryos using the Rice Agilent 44K microarray combined with laser microdissection. Our experimental design and data analysis allowed us to predict expression patterns and changes in the expression of specific genes during key developmental stages and in distinct embryonic organs and domains. In addition, our results point to the key role hormone-related genes and transcription factors play in early embryo development, especially along the apical-basal and dorsal-ventral axes. These findings provide the foundation for future molecular analyses and for increased understanding of spatial gene regulation during rice embryogenesis.

RESULTS

Experimental design and datasets for the microarray

The developmental stages of rice embryogenesis have been previously defined (Itoh et al., 2005b). After fertilization, embryos first show conspicuous morphological changes 3 days after pollination (DAP). However, the shape of embryos at 2 and 3 DAP is ovate and the apical-basal (A-B) embryonic axis is obvious (Fig. 1A,B). At 4 DAP, a protrusion of the coleoptile primordium is found on the ventral side of the embryo, which is the

first morphological change along the dorsal-ventral (D-V) axis. During this stage, differentiation of other embryonic organs, including the shoot apical meristem (SAM), radicle and scutellum are also apparent (Fig. 1C). Accordingly, axis formation and pattern formation of embryos is presumably completed by 3 DAP. Organ differentiation is complete at 7–8 DAP and the embryo reaches its mature shape, although the organs continue to enlarge. At this stage, the primordium of the epiblast (a ventral protrusion from the basal part of the embryo) and a coleorhiza (a tissue enclosing the radicle) are apparent (Fig. 1D).

To acquire a comprehensive transcriptional profile of early embryogenesis in rice, we designed microarray experiments to obtain two datasets: spatial and temporal. For temporal datasets, the entire embryo was collected at 2, 3 and 4 DAP using laser microdissection (LM) (Fig. S1A–C). For spatial datasets, 3-DAP embryos were separated into halves along the A-B and D-V axis using LM (Fig. S1D–G), which resulted in four sets of tissues derived from the apical, basal, dorsal and ventral regions of the embryo (Table 1). In addition to the spatial datasets for early embryos, we obtained embryo tissues closely associated with four embryonic organs at 7 DAP; the shoot, scutellum, root (radicle), and epiblast/coleorhizae, which were separated and collected by LM (Fig. 1D; Fig. S2). These 11 samples were obtained in triplicate and hybridized to the 44K rice microarray (Agilent Technologies), which contains 36,100 independent probes corresponding to 27,370 loci published in RAP-DB (Rice Annotation Project, 2008; Sato et al., 2011) (Table 1). The processed raw signal intensity was subjected to 75th percentile normalization for inter-array comparison. The value was transformed to a log2 scale and the median expression value of the data within each dataset was subtracted for each probe. The processed value was assigned as the normalized expression value. In this study, we used 23,352 probes corresponding to 17,886 loci, with raw signal intensities >50 in at least three of the 33 microarray datasets. Moreover, Pearson correlation analysis with all of the arrays showed high correlation coefficients among the replicates, indicating the reliable quality and reproducibility of the samples (Table S1).

Expression profiles in 3-DAP embryos along the apical-basal and ventral-dorsal axes

To assess the spatial expression profiles of rice embryos prior to morphogenesis, we analyzed spatial datasets derived from four tissues of 3-DAP globular embryos. In our experimental design,

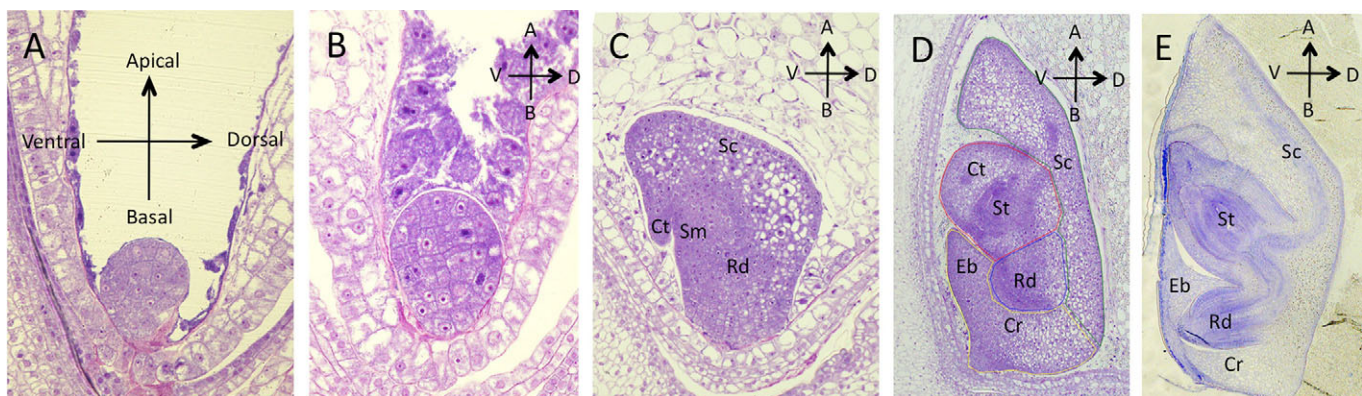


Fig. 1. Embryogenesis of early embryos in rice. (A–E) Morphology of rice embryos during embryogenesis. The putative embryonic axes are indicated in the panels. (A–D) Embryos at 2 (A), 3 (B), 4 (C) and 8 (D) DAP. Colored outlines in red, green, blue and yellow indicate the regions dissected by LM as the shoot, scutellum, root and epiblast/coleorhiza-containing tissues, respectively. (E) Mature embryo. Cr, coleorhiza; Ct, coleoptile; Eb, epiblast; Rd, radicle; Sc, scutellum; Sm, shoot meristem; St, shoot.

Table 1. Embryo stages and tissues collected using LM

Tissue	DAP	Stage*
Temporal dataset		
Whole	2	Early globular (Em3)
Whole	3	Late globular (Em4)
Whole	4	Coleoptiler (Em5)
Spatial dataset		
Apical half	3	Late globular (Em4)
Basal half	3	Late globular (Em4)
Dorsal half	3	Late globular (Em4)
Ventral half	3	Late globular (Em4)
Shoot (ST)	7	Completion of organogenesis (Em7)
Root (RT)	7	Completion of organogenesis (Em7)
Scutellum (SC)	7	Completion of organogenesis (Em7)
Epiblast/coleorhiza (EP)	7	Completion of organogenesis (Em7)

*Stage symbol (in parentheses) defined by Itoh et al. (2005b).

relative expression values for each probe along the A-B axis were assigned by subtracting the normalized expression value of the basal region from that of the apical region. In the same way, relative expression values along the D-V axis were also evaluated by subtracting the ventral values from the dorsal values. Both values were plotted on a scatter diagram with the A-B axis depicted along the y-axis and D-V axis along the x-axis, which represents the

relative expression foci of each probe in the entire 3-DAP embryo (Fig. 2). The pattern of data points for all probes on the scatter diagram was vertically oblong-shaped, indicating that the expression of a greater number of genes was biased along the A-B axis than the D-V axis (Fig. 2A). In addition, we observed a dispersion of the data points on the y-positive area, suggesting that genes for which expression was biased along the D-V axis are enriched in the apical part of the embryo.

To analyze the spatial expression profiles in more detail, we extracted genes preferentially expressed in the four parts of the embryo using moderated *t*-tests (Smyth, 2004) and fold-change analysis [false discovery rate (FDR)<0.05]. Despite the relatively lower threshold of the fold-change (FC) cut-off (FC>2), only 7% of the total expressed genes showed biased expression patterns along the A-B axis; 664 and 960 probes in the apical and basal regions, respectively (Fig. 2B; Table S2). Along the D-V axis, 162 and 81 probes (1% of the total number of expressed genes) showed differential expression between the dorsal and ventral regions, respectively (Fig. 2C; Table S3).

Along both the A-B and D-V axes, 106 probes showed significantly biased expression, and half (54 probes) were found in the apical-ventral region (Fig. 2D; Table S4). Among these, a few genes were detected as conspicuous outliers including: a homolog

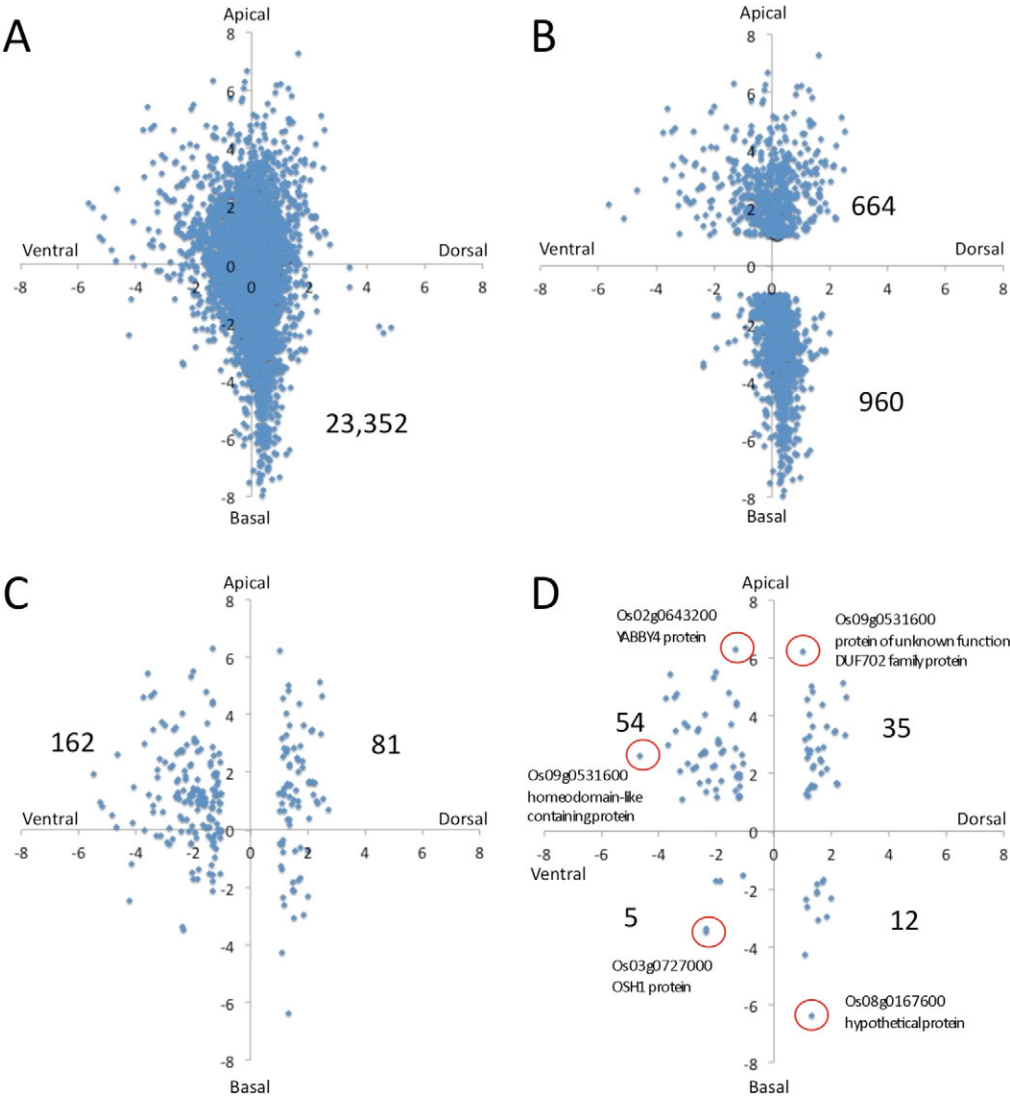


Fig. 2. Spatial expression pattern of genes in 3-DAP embryos. Scatter diagrams depicting gene expression sites in which the position of a dot indicates the virtual expression site of each probe in 3-DAP embryos. x- and y-axes indicate the relative expression values (log2) along the dorsal-ventral and apical-basal axes, respectively. (A) Expression sites of all 23,352 probes examined. (B) Expression sites of genes showing significantly biased expression along the apical-ventral axis [false discovery rate (FDR)<0.05, fold-change (FC)>2]. (C) Expression sites of genes showing significantly biased expression along the dorsal-ventral axis (FDR<0.05, FC>2). (D) Expression sites of genes showing significantly biased expression along both the apical-basal and dorsal-ventral axes (FDR<0.05, FC>2). Red circles indicate probes showing conspicuously biased expression along the apical-basal and/or dorsal-ventral axes, considered to be outliers. The RAP-ID and annotation of the outliers are presented. The number of probes in each group is indicated in the diagram. All data are based on microarray analyses using biological triplicates.

of *Arabidopsis* *STYLISH 1* (Os09g0531600) (Eklund et al., 2010, 2011) in the apical-dorsal region, *OsYABBY4* (Os02g0643200) (Liu et al., 2007; Toriba et al., 2007) and an uncharacterized homeodomain-containing protein (Os04g0566600) in the apical-ventral region, a hypothetical protein (Os08g0167600) in the basal-dorsal region, and *OSH1* (Os03g0727000) in the basal-ventral region (Fig. 2D). The expression pattern of *OSH1* has been reported based on *in situ* hybridization (Sato et al., 1996; Sentoku et al., 1999) (Fig. S7) and was observed in a small domain just below the center of the ventral part of the 3-DAP embryo, in agreement with our *in silico* prediction.

Relationship between temporal changes and spatial expression patterns in the globular embryo

To understand the relationship between temporal dynamics and spatial patterns of gene expression, we first categorized the expressed genes that showed fluctuating expression levels during early embryogenesis (12,232 probes) into eight groups (E1–E8) based on the similarity of expression patterns in the temporal dataset using K-means clustering algorithms (Fig. S3A). Next, we extracted probes that were significantly biased along the A-B and D-V axes of the spatial datasets at 3 DAP (Fig. 2B,C) from the eight clusters. The total number of extracted probes preferentially expressed in the apical, basal, dorsal and ventral regions was 552, 635, 67 and 130, respectively. We then examined the spatial expression patterns of the extracted probes using a scatter diagram for each cluster (Fig. S3B; Table S5), and calculated the percentage of the extracted probe compared with the total number of preferentially expressed probes in the apical, basal, dorsal and ventral region in each cluster (Fig. S3C; Table S6).

Generally, nearly 80% of genes were expressed similarly across the three stages and comprised expression groups E2, E4 and E6 yielding 38.6%, 13.4% and 27.0% of the total expressed genes (Fig. S3D). The percentage of genes showing biased expression patterns either along the A-B or D-V axis in these groups was low (Fig. S3D). For example, the E2 expression cluster represented 38.6% of the total expressed genes, but only a small subset were preferentially expressed, i.e. 17.0% (94/552) in the apical region, 14.0% (89/635) in the basal region, 14.9% (10/67) in the dorsal region and 11.5% (15/130) in the ventral region. By contrast, genes categorized into groups E3, E5 and E7 showed relatively larger expression changes during early embryogenesis (Fig. S3A). These groups contained a small proportion of expressed genes, but were greatly enriched in genes that were preferentially expressed along the A-B and D-V axes. In particular, the gene cluster E5 comprised only 2.9% of the total analyzed genes, yet many of these genes showed biased expression in the apical, basal, dorsal and ventral regions; 21.4%, 8.5%, 23.9% and 27.7%, respectively (Fig. S3D). These results suggest a correlation between temporal changes and spatial patterns of gene expression during embryogenesis.

Spatial distribution of phytohormone-related genes

Although it has been reported that auxin and cytokinin are important phytohormones for embryonic patterning and cell specification during early embryogenesis in *Arabidopsis* (Müller and Sheen, 2008; Möller and Weijers, 2009), limited information is available on the roles of auxin and cytokinin during early embryogenesis in rice. In addition, the roles of other phytohormones during rice embryogenesis remains limited. Therefore, we analyzed the spatial distributions of phytohormone-related genes in 3-DAP embryos (Fig. 3; Table S7). The scatter diagrams for expression of phytohormone-related genes revealed that few genes showed biased

expression patterns, although no consistent pattern for all data points was observed among the six phytohormones in 3-DAP embryos. Accordingly, the polarized biosynthesis, catabolism and signaling of phytohormones by a limited number of genes might contribute to developmental or physiological processes in globular embryos.

Analysis of gibberellin (GA)-related genes (Fig. 3A) revealed that *OsSLRL1*, a GRAS protein that functions as a repressor of GA signaling (Itoh et al., 2005a), was preferentially expressed in the basal region. Although *OsSLRL1* is highly expressed in inflorescence meristems and reproductive organs (Itoh et al., 2005a), the function of *OsSLRL1* in embryogenesis was previously unknown. We also found that *OsGA20ox1*, a GA biosynthesis gene, is expressed in the apical-dorsal region in 3-DAP embryos. Although bioactive GAs synthesized at the epithelium during germination are essential to induce α -amylase expression in the endosperm, the role of polarized expression of GA-related genes during early embryogenesis remains unclear.

The auxin-related genes *OsIAA7* and *OsARF10* were expressed in the apical and basal region (Fig. 3B). It has been shown that not only auxin biosynthesis and signaling but also polar auxin efflux is important for auxin-dependent developmental processes during embryogenesis (Friml et al., 2003; Möller and Weijers, 2009). *Arabidopsis* PIN1, PIN3, PIN4 and PIN7 are required to establish apical-basal polarity via directional auxin transport during embryogenesis (Friml et al., 2003). Thus, we examined the expression data of rice PIN-like genes and presented them in a scatter diagram (Fig. S4). Some PIN-like genes showed polarized expression along the A-B axis. However, the rice PIN-like genes exhibiting the most polarized expression were homologous to PIN2, PIN5 and PIN8 (Wang et al., 2009), which do not have dominant functions in embryogenesis in *Arabidopsis*. Although accumulation patterns and localization of PIN1 proteins during embryogenesis were observed in maize (Forestan et al., 2010), it is important to identify the PIN-like genes that participate in auxin-dependent processes during early embryogenesis in rice.

We also identified three cytokinin (CK) A-type response regulator genes, *OsRR5*, *OsRR6* and *OsRR11*, that were preferentially expressed in the apical-ventral region (Fig. 3C). They were closely related and are believed to be negative regulators of CK signaling (Hirose et al., 2007). Their closest homolog in maize is the *ABPH1* gene, which is known to play a role in the establishment of phyllotaxy by maintaining SAM size and PIN expression. It is specifically expressed in the SAM during embryogenesis (Giulini et al., 2004; Lee et al., 2009). Accordingly, the three response regulator genes detected in the apical-ventral region were required for SAM establishment before morphogenesis.

The brassinosteroid (BR)-related genes *OsDET2* and *OsBAS1L1* are possibly involved in BR biosynthesis and inactivation, respectively, and were found to be expressed in the basal region (Fig. 3D). The BR receptor-like protein *OsBRL1*, which is partially associated with BR perception, was also preferentially expressed in the basal region. Because *OsBRL1* was mainly expressed in roots (Nakamura et al., 2006), the expression of *OsBRL1* in the basal region might be associated with radicle development during early embryogenesis.

Amongst ethylene- and abscisic acid (ABA)-related genes (Fig. 3E,F), few showed biased expression patterns. For example, biosynthesis genes for ethylene and ABA were expressed in the basal region of the embryo (Fig. 3E). However, it is unknown whether these plant hormones are associated with early embryogenesis. Future studies will explore how these genes are involved in the regulation of early embryogenesis.

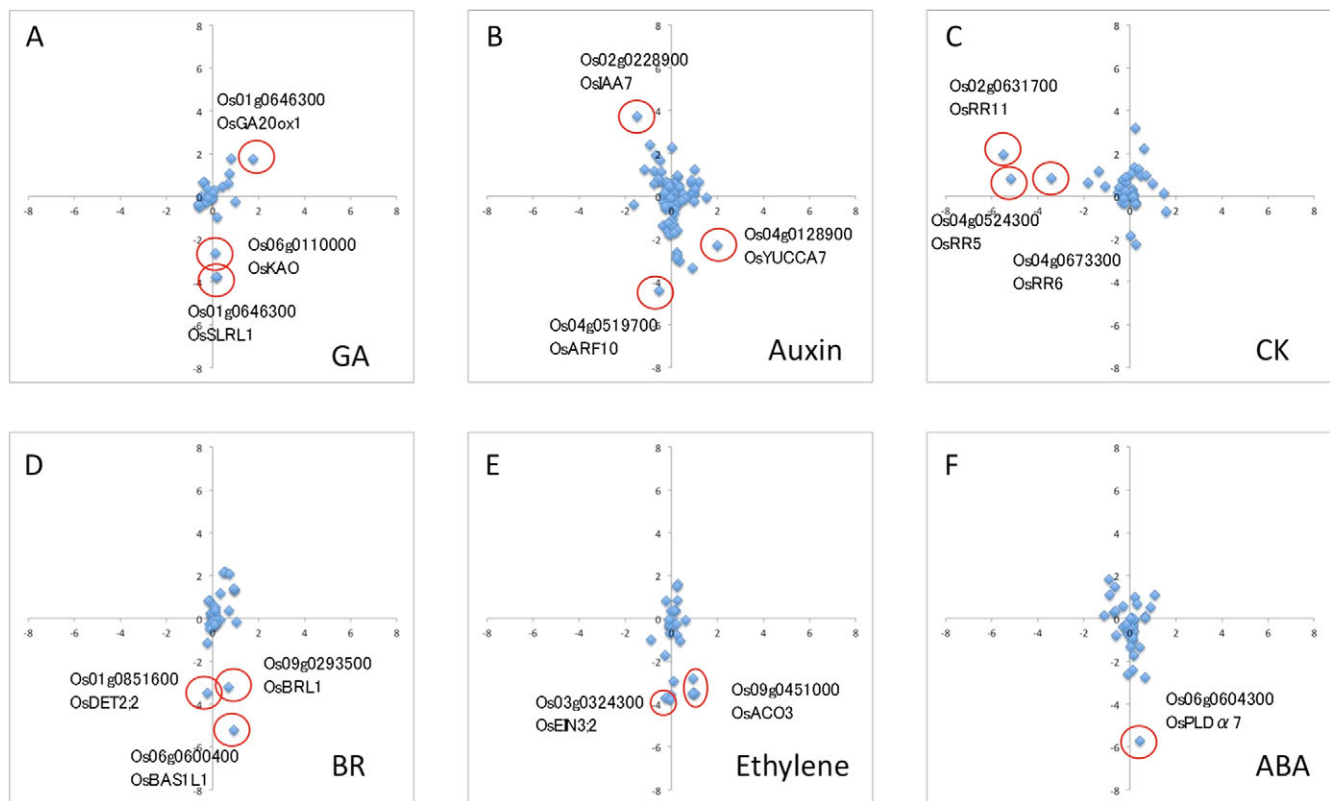


Fig. 3. Spatial distribution of phytohormone-related genes. (A–F) Scatter diagrams depicting expression sites of phytohormone-related genes expressed in 3-DAP embryos. x- and y-axes indicate the relative expression values (log2) along the dorsal-ventral and apical-basal axes, respectively. Red circles indicate probes that showed conspicuously biased expression along the dorsal-ventral and/or apical-basal axes, considered to be outliers. The RAP-ID and annotations of the outliers are presented. ABA, abscisic acid; BR, brassinosteroid; CK, cytokinin; GA, gibberellin. All data are based on microarray analyses using biological triplicates.

Spatial distribution of transcription factors and transcriptional regulator genes

Transcription factors (TFs) and transcriptional regulators (TRs) are known to play crucial roles in various developmental and physiological processes during embryogenesis. Thus, we analyzed the spatial expression of TF and TR genes in 3-DAP embryos. TF and TR genes in rice have been categorized into dozens of families (Pérez-Rodríguez et al., 2010) (Table 2). Scatter diagrams of the 43 TF and TR families containing more than ten probes were analyzed (Table S8). We found that data point patterns were considerably different among the TF and TR families. We then categorized TF and TR families into three groups according to the degree of dispersion of the data points, and three examples of each category with the plots of several outliers are shown in Fig. 4. Type I represents TF and TR families in which >20% of genes show higher absolute relative expression values [$AREV = (x^2 + y^2)^{1/2}$] > 2.0, or, more specifically, more genes showing biased expression from the center of the embryo (Table 2). OFP (ovate family protein), LOB (lateral organ boundaries), C2C2-Dof, C2C2-YABBY, GRF (growth regulating factor), HB (homeobox), MADS (MCM1, AGAMOUS, DEFICIENS and SRF), TCP (TB1, CYC and PCFs), AUX/IAA (auxin/indole-3-acetic acid) and bHLH (basic helix-loop-helix) families were categorized in this group. For example, more than half of the OFP genes showed polarized expression patterns with AREVs > 2 (Fig. 4A). Similarly, about half of C2C2-Dof genes showed biased expression patterns, and their expression was preferentially detected in the apical region of the embryo (Fig. 4B). HB genes belong to the second-largest gene family, and

22 HB probes showed AREVs > 2. Among them, *OSH1* and an uncharacterized *WOX* gene (Os07g0684900, Os05g0564500), which are closely related to *WOX11/WOX12* and *WOX8/WOX9* in *Arabidopsis* (Dai et al., 2007; Nardmann et al., 2007), showed more deviated expression patterns (Fig. 4C).

The TF and TR families in Type II contain only a few genes with biased expression patterns (Table 2; Fig. 4D–F). A total of 19 TF and TR families, such as AP2-EREBP (which is the largest TF family), bZIP (basic leucine zipper) and NAC (NAM, ATAF and CUC) were included in these families. In AP2-EREBP, a homolog of *ESR/DRN* that is known to be a developmental regulator of embryogenesis in *Arabidopsis* (Chandler et al., 2007; Cole et al., 2009) and an uncharacterized ERF/AP2 gene (Os02g0657000) exhibited deviated expression patterns (Fig. 4D). Similarly, two genes, *OsNAM*, a rice homolog of *Arabidopsis CUC1*, which is involved in shoot meristem formation (Hibara and Nagato, 2005), and *OsNAC7*, a homolog of *SOMBRERO (SMB)* involved in root cap development in *Arabidopsis* (Bennett et al., 2010), were expressed with polarized patterns, but the majority of other NACs were not (Fig. 4F).

A total of 13 TF and TR families were categorized into Type III (Table 2; Fig. S5). Data points of the genes in this group showed a concentrated pattern towards the center of the scatter diagram, suggesting that the expression of these genes was uniform. Six of eight TR families were categorized as Type III, suggesting that spatial regulation of TR families might be less important than that of TF families, excluding AUX/IAA and TRAF (BTB/POZ domain-containing protein) families (Table 2).

Table 2. Spatial distribution of transcription factor and transcriptional regulator genes in 3-DAP embryos

Name of TF/TR [‡]	Number of probes expressed in 3-DAP embryos	Number of probes with AREV >2	Percentage of probes with AREV >2	TF or TR [‡]
Type I*				
OFP	18	10	55.6	TF
LOB	16	8	50.0	TF
C2C2-Dof	17	8	47.1	TF
C2C2-YABBY	12	5	41.7	TF
GRF	11	4	36.4	TF
HB	110	37	33.6	TF
MADS	49	14	28.6	TF
TCP	19	5	26.3	TF
AUX/IAA	32	8	25.0	TR
bHLH	73	17	23.3	TF
Type II*				
ABI3VP1	26	5	19.2	TF
AP2-EREBP	119	22	18.5	TF
C2H2	57	9	15.8	TF
Trihelix	19	3	15.8	TF
WRKY	45	7	15.6	TF
C2C2-GATA	21	3	14.3	TF
Orphans	46	5	10.9	TF
G2-like	29	3	10.3	TF
TRAF	21	2	9.5	TR
MYB-related	66	6	9.1	TF
MYB	60	5	8.3	TF
HSF	37	3	8.1	TF
ARF	38	3	7.9	TF
NAC	52	4	7.7	TF
bZIP	82	6	7.3	TF
GRAS	42	3	7.1	TF
SBP	14	1	7.1	TF
FHA	19	1	5.3	TF
CCAAT	47	2	4.3	TF
C3H	74	1	1.4	TF
Type III*				
Alfin-like	13	0	0.0	TF
BSD	11	0	0.0	TF
E2F-DP	11	0	0.0	TF
FAR1	33	0	0.0	TF
GNAT	26	0	0.0	TR
HMG	11	0	0.0	TR
Jumonji	13	0	0.0	TR
mTERF	28	0	0.0	TF
PHD	47	0	0.0	TR
SET	34	0	0.0	TR
SNF2	38	0	0.0	TR
Tify	12	0	0.0	TF
TUB	22	0	0.0	TF

AREV, absolute relative expression value.

*Types are categorized based on the percentage of probes with AREV >2.

Types I, II and III are the TF and TR families containing >20%, 0–20%, and 0% sites with AREV >2, respectively.

[‡]TF and TR families are categorized using the Plant Transcription Factor Database (<http://plntfdb.bio.uni-potsdam.de/v3.0/>).

These analyses revealed that the spatial distribution of gene expression was significantly different between the TF families. TF families in Type I, such as HB and YABBY, include putative homologs of well-known developmental regulators expressed in specific parts of early embryos in *Arabidopsis* (Capron et al., 2009). By contrast, Type I TF families also contained genes for which functions in embryogenesis remain unknown, even in *Arabidopsis*. In particular, more than half of the OFP genes showed

highly biased expression patterns in 3-DAP embryos (Fig. 4A). Although OFP family members play multiple roles in developmental processes as transcriptional repressors, and few members of the *Arabidopsis* OFP family are known to interact with KNOX proteins (Li et al., 2011), further analysis of OFP genes is required to examine their involvement in embryo development. C2C2-Dof proteins were involved in various aspects of development, growth, and environmental response. The majority of *Arabidopsis* Dof genes were expressed in vascular tissues (Le Hir and Bellini, 2013). Some rice C2C2-Dof genes were expressed in the center of the apical region (Fig. 4B), suggesting that they are associated with early vascular development or specification in rice embryos.

Only a few genes in the Type II TF families showed biased expression patterns. In the case of NAC genes, *OsNAM* and *OsNAC7* showed highly polarized expression patterns (Fig. 4F); homologs of these genes in *Arabidopsis* are known to be involved in shoot and root development, respectively. It is interesting that genes showing biased expression patterns in rice are orthologs of important developmental regulators in *Arabidopsis*, such as *CUC1*, *SMB* and *ESR/DRN*. Accordingly, spatial expression-based functional analysis will be used to explore the roles of uncharacterized TF genes in embryonic development.

Relationship between expression profiles in globular embryo and later embryonic stages

To examine the relationship between the expression patterns of genes in globular embryos and embryos in the later stages, we investigated expression profiles in four embryonic organs; i.e. shoot, scutellum, root (radicle), and epiblast/coleorrhizae-containing tissues at 7 DAP. We identified genes for which expression values in one region of 7-DAP embryos were twofold higher than in the other three regions; these were defined as tissue-specific upregulated genes. ANOVA (FDR<0.05) revealed that 12,403 probes were differentially expressed among shoot, scutellum, root (radicle) and epiblast/coleorrhiza-containing tissues at 7 DAP. Among the 12,403 probes, 393, 593, 401 and 453 were detected as tissue-specific upregulated genes in shoot, scutellum, root, and epiblast tissues, respectively (Table S9).

We next analyzed the spatial pattern of expression of these tissue-specific upregulated genes and calculated the barycenter of the data points in 3-DAP embryos (Fig. S6). Data points of shoot-specific genes were broadly scattered in the apical-ventral region. The barycenter of shoot-specific upregulated genes was located in the *x*-negative and *y*-positive area. Thus, genes specifically expressed in the shoot at 7 DAP tended to be expressed in the apical-ventral region of 3-DAP embryos. The pattern of data points of scutellum-specific upregulated genes was similar to that of shoot-specific upregulated genes, but more genes were detected in the apical-dorsal region. By contrast, global expression bias along the D-V axis was not observed in root-specific upregulated genes, and the barycenter of root-specific upregulated genes was relatively close to the origin of the diagram, indicating that many genes specifically expressed in the root tissue showed uniform or centered expression in 3-DAP embryos. The epiblast-specific upregulated genes were more concentrated in the basal region with a narrow range along the D-V axis, and the barycenter was located in the *y*-negative area near the *x*-axis. The relative positions of the barycenters for the four tissues in 3-DAP embryos corresponded to the relative positions of the organs in 7-DAP embryos.

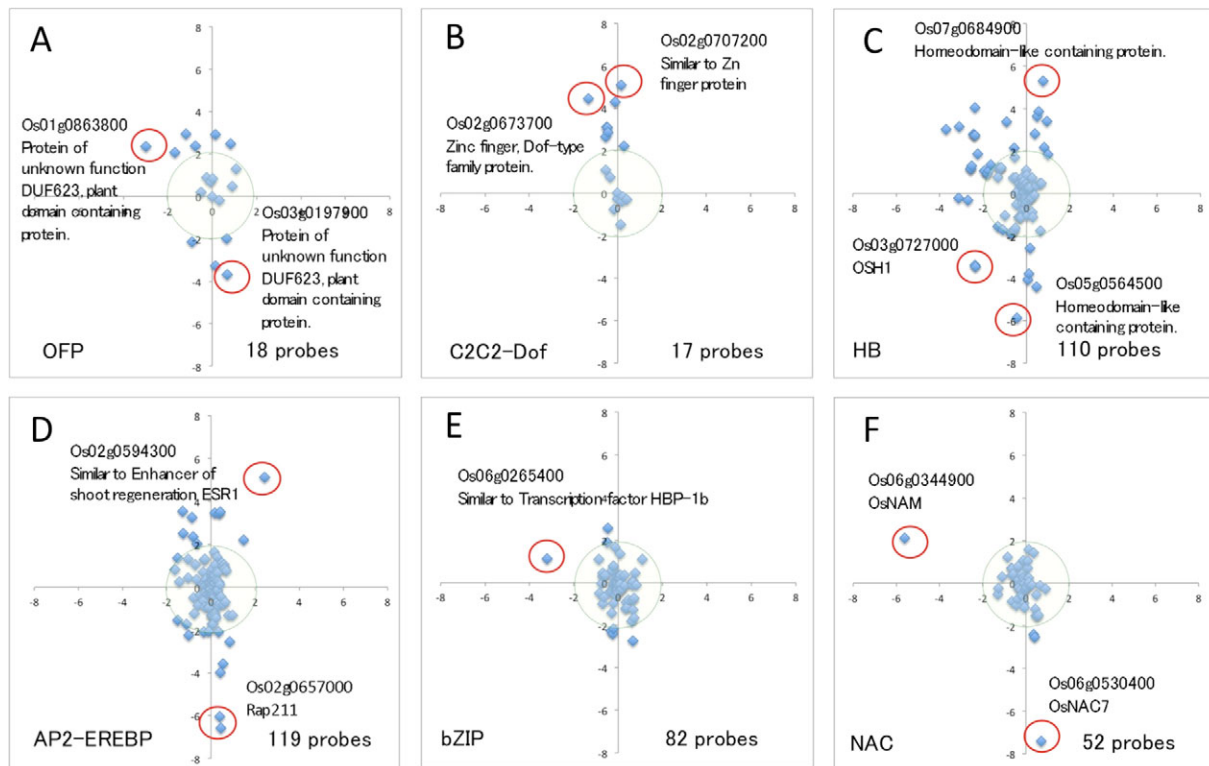


Fig. 4. Spatial distribution of transcription factor and transcriptional regulator genes. Scatter diagrams depicting sites of transcription factor (TF) and transcriptional regulator (TR) genes expression in 3-DAP embryos. x- and y-axes indicate the relative expression values (log2) along the dorsal-ventral and apical-basal axes, respectively. Data points inside the green circle represent probes with absolute relative expression values of <2. Red circles indicate probes that showed conspicuously biased expression along the dorsal-ventral and/or apical-basal axes, considered to be outliers. The RAP-ID and annotations of outliers are presented. TFs and TRs are categorized as Type I (A–C) or II (D–F) (see text and Table 2). All data are based on microarray analyses using biological triplicates.

Confirmation of gene expression patterns using *in situ* hybridization

To verify whether our microarray analyses of expression patterns were consistent with actual expression patterns, *in situ* hybridization experiments were performed with 55 genes expressed in a polarized pattern along the A–B and D–V axes. These genes were randomly selected using the following criteria: raw signal intensity >200, annotated gene functions, and cloned full-length transcripts (Table S10). In addition to the expression pattern at 3 DAP, we also examined the pattern at 4 DAP to evaluate changes from 3 DAP to 4 DAP. Expression patterns of most genes in 3-DAP embryos were consistent with the expression domain based on the microarray data, although some genes showed weak and uniform expression patterns (Fig. 5; Fig. S7). We selected examples of genes showing specific spatial expression patterns (Fig. 5). The Os06g0130100 gene was similar to *ERL1* and *ERL2* in *Arabidopsis* (Shpak et al., 2004), and its expression was strongly detected in the apical region of both 3- and 4-DAP embryos (Fig. 5A). The microarray data indicated that this gene should be expressed in the apical region of the 3-DAP embryo (Fig. 5A, scatter diagram). Similarly, Os03g0244600, encoding an AUX1-like protein, was predicted to be in the apical region of the 3-DAP embryo; however, expression of the gene was detected in the center of the 3-DAP embryo and in the pre-vascular domain of the 4-DAP embryo (Fig. 5B). The microarray data indicated that Os02g0614300 (Fig. 5C), Os09g0451000 (Fig. 5D), Os06g0520600 (Fig. 5E) and Os01g0691100 (Fig. 5F) were similarly expressed in the basal region of the 3-DAP embryo. *In situ* hybridization revealed that these genes were expressed in the center (Fig. 5C), a small domain

(Fig. 5D), a broad domain (Fig. 5E), as well as a few layers of the basal region (Fig. 5F) in 3-DAP embryos. The difference in expression patterns among the genes was more apparent in 4-DAP embryos. Os06g0265400 (Fig. 5G) was expressed in a few cells on the ventral side of the apical embryo and in the tip of presumptive coleoptile primordium at 4 DAP. Although Os01g0954500 (Fig. 5H) was annotated as an unknown protein, it encodes a protein homologous to *LATERAL ROOT PRIMORDIUM 1* in *Arabidopsis* (Smith and Fedoroff, 1995). Expression of this gene was detected on the dorsal side of 3-DAP embryos and in the scutellum of 4-DAP embryos. Taken together, these results indicate that our transcriptional profiling of early embryogenesis was reliable, and that clustering based on the expression domains might facilitate screening for marker genes for embryogenesis in rice.

DISCUSSION

In summary, we report herein the spatiotemporal transcriptome of embryogenesis in rice. The spatial data sets of 3-DAP embryos allowed us to predict the spatial bias of gene expression along the A–B and D–V axes in the globular embryo. Our data also showed temporal changes in the expression levels and sites of individual genes from globular to pre-mature embryos. The analysis suggests that the expression of a small number of genes is polarized along the A–B and D–V axes in the globular embryo, and that the expression level of these polarized genes tends to fluctuate depending on the developmental stage. This indicates that only a small number of expressed genes are polarized in the rice globular embryo, and a greater number of those genes show biased expression patterns

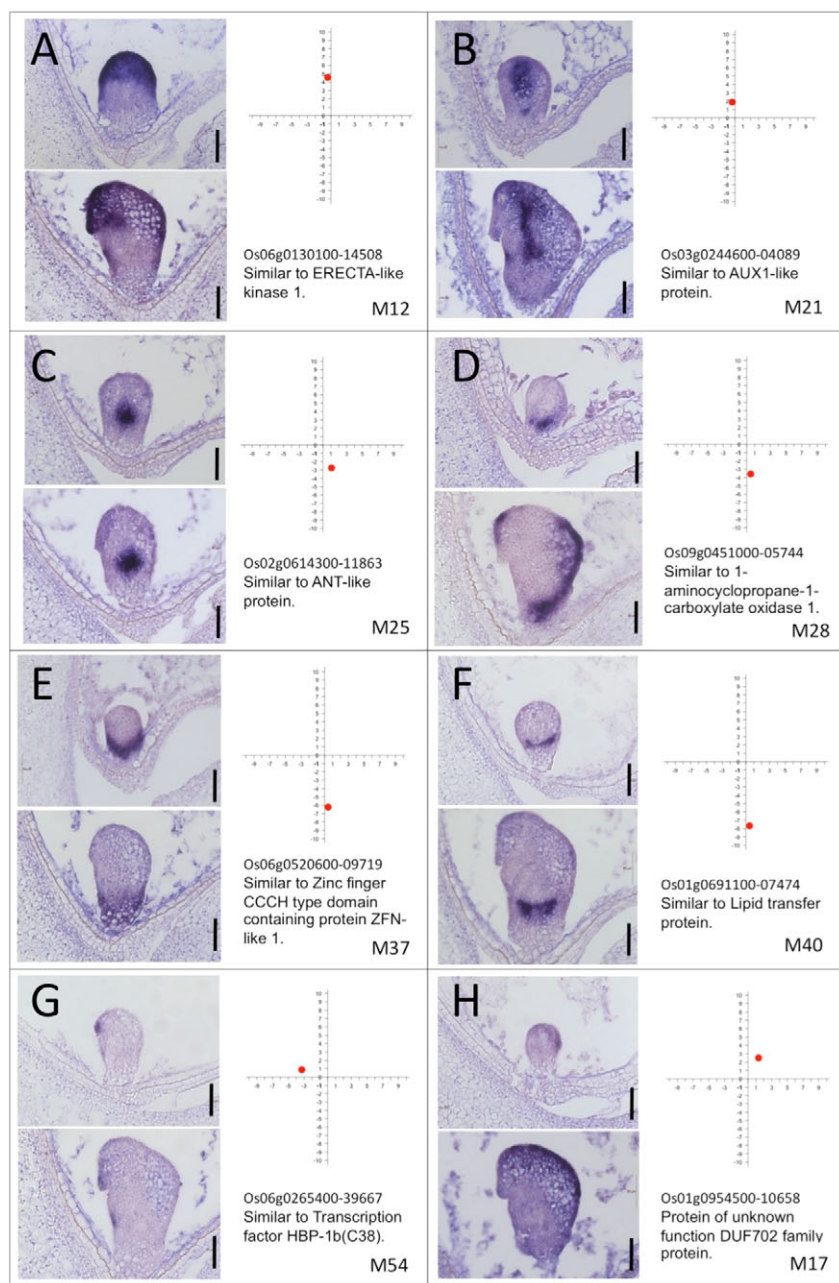


Fig. 5. Spatial expression patterns of several potential marker genes. Upper and lower images of each panel show the expression patterns of 3- and 4-DAP embryos, respectively, for Os06g0130100 (A), Os03g0244600 (B), Os02g0614300 (C), Os09g0451000 (D), Os06g0520600 (E), Os01g0691100 (F), Os06g0265400 (G) and Os01g0954500 (H). The scatter diagrams indicate the predicted expression site of the corresponding probe based on microarray analysis. *x*- and *y*-axes indicate the relative expression values (log2) along the dorsal-ventral and apical-basal axes, respectively. The RAP-ID, probe number, annotations and marker ID (see Table S10) of the genes are indicated. Scale bars: 50 μ m.

along the A-B axis than the D-V axis. Considering that the globular embryo at 3 DAP showed no morphological changes along the D-V axis, the small number of genes showing polarized expression along the D-V axis must be required for successful morphogenesis and establishment of the D-V axis.

The spatial distribution of phytohormone-related genes suggests that a few genes related to each phytohormone show embryonic axis-dependent expression. For example, our finding that *OsGA20ox1* is expressed in the apical-dorsal region of 3-DAP embryos is consistent with a previous report that *OsGA20ox1* is expressed in the epithelium of the scutellum (Kaneko et al., 2003). Strikingly, our analysis of auxin efflux PIN genes revealed that rice homologs of PIN2, PIN5 and PIN8 were the only PINs showing polarized expression in the rice embryo, which differs from *Arabidopsis* embryogenesis. Interestingly, a rice homolog of the maize *ABPH1* gene was preferentially expressed in the apical ventral region of the

embryo, suggesting a role for cytokinin A-type response regulators in regulating rice embryonic SAM formation and perhaps PIN expression. We also identified an *OsBRL1* gene preferentially expressed in the basal region; interestingly, BR perception is known to be important for root development (Nakamura et al., 2006). We did not detect many ABA- or ethylene-related genes with polarized or biased expression in the embryo with the exception of a few biosynthesis genes. Although the roles of most of the phytohormone-related genes in embryogenesis remains unknown, future functional characterization of some of the genes described in this study should confirm their importance during rice early embryogenesis.

The spatial gene expression patterns of TF and TR families differed significantly, indicating that specific TF families might contribute to early patterning of the embryo. The expression bias in the globular embryo was weakly related to the expression level of

the embryonic organs at later stages, suggesting that organ-specific programs are initiated before morphogenesis.

Overall, these analyses indicated that genetic programs required for embryonic organ function are initiated in globular embryos, and the relative positions of the embryonic organs are determined during this stage. It is not surprising that gene expression patterns at 3 DAP are associated with those at 7 DAP, but the spatial correlation between them was not as tight as expected. This suggested that the spatial expression of a number of genes can be significantly changed after morphogenesis (e.g. Fig. 5D). In addition, root-specific upregulated genes were observed around the center of 3-DAP embryos. Accordingly, only a few genes are known to be involved with root development and function, e.g. *OsNAC7* and *OsBRL1*, and were expressed in the basal region (Fig. 4F; Fig. 3D). This indicates that the majority of genes associated with root function are probably activated in the center of the embryo at 3 DAP. This is consistent with the fact that the root primordium is formed endogenously near the center of the early embryo in grasses, unlike the *Arabidopsis* embryonic root, which differentiates at the basal part of the embryo proper during the globular stage (Chandler et al., 2008).

Furthermore, we confirmed the accuracy of the expression patterns identified by microarray analysis using *in situ* hybridization, and found several genes expressed in a specific domain during early embryogenesis. However, we also found that some genes showing preferential expression in the microarray analysis did not always show similar expression patterns by *in situ* hybridization (e.g. Os06g0520600 and Os01g0691100; Fig. 5E,F). One reason for this is that our experimental design cannot distinguish between gradients of expression levels in the radial direction. Further analysis using centric tissues of the 3-DAP embryos along the radial direction can be used to increase the accuracy of expression domains, which will be used to establish a ‘digital *in situ* expression’ database in 3-DAP embryos of rice, similar to previous high-resolution expression analyses performed with *Arabidopsis* roots (Brady et al., 2007). Finally, expression data were deposited in the expression profile database, RiceXPro (http://ricexpro.dna.affrc.go.jp/RXP_4002/index.php) (Sato et al., 2011, 2013), and can be accessed in the form of raw and normalized expression graphs and expression site graphs similar to electronic fluorescent pictographs seen in other databases (Winter et al., 2007) (Fig. S8).

Our transcriptome study serves as a foundation for the functional analysis of genes regulating rice embryogenesis and for understanding the diversity and conservation of genetic programs of embryogenesis by establishing common and different genetic landmarks for embryogenesis in various plant species.

MATERIALS AND METHODS

Plant materials and growth conditions

Rice (*Oryza sativa* L. japonica cv. Nipponbare) plants were grown in a paddy field under normal conditions. Ovaries at 2, 3, 4 and 7 DAP were collected.

Sample preparation

For plastic sections, the collected ovaries were fixed in a 1:1:18 solution of formaldehyde, acetic acid and 50% ethanol for 24 h at 4°C. After dehydration in a graded ethanol series, samples were embedded in Technovit 7100 (Heraeus Kulzer) and cut into 3-μm-thick sections with a microtome. Sections were stained with Toluidine Blue.

For LM, ovaries at 2, 3, 4 and 7 DAP were fixed in pre-chilled solution of 75% ethanol/25% acetate with vacuum infiltration. Paraffin embedding was performed using a microwave processor (Energy Beam Sciences) according to Takahashi et al. (2010). Paraffin-embedded samples were cut

into 10-μm-thick sections using a microtome (RM2255; Leica). Laser microdissection was performed using the Veritas Laser Microdissection System LCC1704 (Arcturus, now Life Technologies).

For *in situ* hybridization, samples were fixed in 4% paraformaldehyde in 0.1 M sodium phosphate buffer for 24 h at 48°C, and then dehydrated in a graded ethanol series. The ethanol was replaced with xylene and the samples were embedded in Paraplast Plus (Leica). Paraffin sections (8 mm thick) were applied to microscope slides coated with 3-aminopropyl triethoxysilane (Matsunami Glass). To generate probes for 55 genes (see Table S10), the corresponding full-length cDNA clones deposited in the NIAS Genebank (<http://www.dna.affrc.go.jp/distribution/>) were ordered and used as templates. The full-length cDNA fragments were amplified by PCR and then transcribed using digoxigenin-labeled antisense riboprobes using a MAXIscript In Vitro Transcription Kit (Life Technologies) with digoxigenin-11-UTP (Roche).

RNA extraction and microarray analysis

RNA extraction and microarray analysis were performed according to Takehisa et al. (2011). Briefly, total RNA was extracted from the collected samples with a Pico-Pure RNA isolation kit (Arcturus, now Molecular Devices), and the Cy3-labeled cRNA was purified using the RNeasy Mini Kit (Qiagen). A total of 1000 ng Cy3-labeled cRNA was fragmented and hybridized on a slide of rice 4×44K microarray RAP-DB (G2519F#15241; Agilent Technologies). After washing, slides were scanned on an Agilent G2505B DNA microarray scanner, and background correction of the raw Cy3 signals was performed using the Feature Extraction 10.5.1.1 software (Agilent Technologies).

Statistical analysis

Normalization procedures were performed using 75th percentile normalization for inter-array comparison and baseline correlation to the median of data within each dataset using GeneSpringGX12. The processed value was used as a normalized expression value. In addition, Pearson correlation analysis with all of the arrays using normalized data for looking at similarity between replicates was performed in Excel (Microsoft). In this study, we used 23,352 probes corresponding to 17,886 loci, with raw signal intensities >50 in at least three of the 33 microarray datasets. Differentially expressed genes between apical and basal and between dorsal and ventral tissue in 3-DAP embryos were statistically identified using moderated *t*-tests (Smyth, 2004), and fold-change analysis was performed using GeneSpringGX12. *P*-values were adjusted for multiple testing using Benjamini and Hochberg’s method for correcting FDR. The relative expression values along the A-B axis and the D-V axis were calculated by subtracting the normalized expression values of the basal region from those of the apical region, and those of the ventral region from the dorsal region, respectively. Scatter diagrams of spatial expression profiles in 3-DAP embryos were constructed in Excel. Differentially expressed genes among the temporal data set were categorized into eight clusters using K-means cluster analyses based on a Euclidean algorithm with GeneSpringGX12. For extraction of differentially expressed genes in the temporal data set (whole embryo at 2, 3 and 4 DAP) and the sub-spatial data sets [shoot, scutellum, root (radicle) and epiblast-coleorrhizae-related tissues at 7–8 DAP], we performed ANOVA (FDR<0.05) and fold-change analyses using the relative expression values in each dataset.

Gene annotation used for analyses

The gene annotation used in this study was obtained from the RAP-DB (Rice Annotation Project, 2008). The list of genes associated with biosynthesis, catabolism and signaling for the six phytohormones described here was derived from Hirano et al. (2008). For extraction of transcription factor and transcriptional regulator genes from the rice genome, the list in the Plant Transcription Factor Database (Pérez-Rodríguez et al., 2010; <http://plntfdb.bio.uni-potsdam.de/v3.0/>) was used.

Acknowledgements

We would like to thank Ms Ritsuko Motoyama [National Institute of Agrobiological Sciences (NIAS)] for microarray analysis and Ms Minami Omae (Nagoya University) for help with *in situ* hybridization experiments. We also thank Ms Kaori Kamatsuki

(Mitsubishi Space Software) for helping with the database construction and Ms Hisae Kamakura (NIAS) for help with laser microdissection experiments.

Competing interests

The authors declare no competing or financial interests.

Author contributions

J.-I.I., Y.S. (NIAS) and H.T. prepared samples, performed laser microdissection, isolated RNA, analyzed data. Y.S. (Nagoya University) and S.S.-S. performed *in situ* hybridizations. K.-I.H. and H.K. made histological sections of embryos. N.N. contributed to the database construction. J.-I.I., K.A.S. and Y.S. (NIAS) wrote the article. J.-I.I., Y.S., Y.S., K.-I.H. and Y.N. contributed to the design of the research.

Funding

This work and the database construction of this work was supported mainly by a project of the Ministry of Agriculture, Forestry and Fisheries of Japan (Genomics for Agricultural Innovation, RTR0002, RTR0006, and Development of Genome Information Database System for Innovation of Crop and Livestock Production), and partly by a grant from a Grant-in-Aid for Scientific Research from the Ministry of Education, Culture, Sports, Science and Technology of Japan [24380005 to J.I.].

Data availability

The data obtained in this study have been deposited in the National Center for Biotechnology Information (NCBI) Gene Expression Omnibus (GEO), and are accessible through accession number (GSE63110).

Supplementary information

Supplementary information available online at

<http://dev.biologists.org/lookup/suppl/doi:10.1242/dev.123661/-/DC1>

References

- Belmonte, M. F., Kirkbride, R. C., Stone, S. L., Pelletier, J. M., Bui, A. Q., Yeung, E. C., Hashimoto, M., Fei, J., Harada, C. M., Munoz, M. D. et al. (2013). Comprehensive developmental profiles of gene activity in regions and subregions of the *Arabidopsis* seed. *Proc. Natl. Acad. Sci. USA* **110**, E435–E444.
- Bennett, T., van den Toorn, A., Sanchez-Perez, G. F., Campilho, A., Willemsen, V., Snel, B. and Scheres, B. (2010). *SOMBRERO*, *BEARSKIN1*, and *BEARSKIN2* regulate root cap maturation in *Arabidopsis*. *Plant Cell* **22**, 640–654.
- Brady, S. M., Orlando, D. A., Lee, J.-Y., Wang, J. Y., Koch, J., Dinneny, J. R., Mace, D., Ohler, U. and Benfey, P. N. (2007). A high-resolution root spatiotemporal map reveals dominant expression patterns. *Science* **318**, 801–806.
- Breuninger, H., Rikirsch, E., Hermann, M., Ueda, M. and Laux, T. (2008). Differential expression of *WOX* genes mediates apical-basal axis formation in the *Arabidopsis* embryo. *Dev. Cell* **14**, 867–876.
- Capron, A., Chatfield, S., Provart, N. and Berleth, T. (2009). Embryogenesis: pattern formation from a single cell. *Arabidopsis Book* **7**, e0126.
- Casson, S., Spencer, M., Walker, K. and Lindsey, K. (2005). Laser capture microdissection for the analysis of gene expression during embryogenesis of *Arabidopsis*. *Plant J.* **42**, 111–123.
- Chandler, J. W., Cole, M., Flier, A., Grewe, B. and Werr, W. (2007). The AP2 transcription factors DORNROSCHE and DORNROSCHE-LIKE redundantly control *Arabidopsis* embryo patterning via interaction with PHAVOLUTA. *Development* **134**, 1653–1662.
- Chandler, J., Nardmann, J. and Werr, W. (2008). Plant development revolves around axes. *Trends Plant Sci.* **13**, 78–84.
- Chen, J., Zeng, B., Zhang, M., Xie, S., Wang, G., Hauck, A. and Lai, J. (2014). Dynamic transcriptome landscape of maize embryo and endosperm development. *Plant Physiol.* **166**, 252–264.
- Cole, M., Chandler, J., Weijers, D., Jacobs, B., Comelli, P. and Werr, W. (2009). DORNROSCHE is a direct target of the auxin response factor MONOPTEROS in the *Arabidopsis* embryo. *Development* **136**, 1643–1651.
- Dai, M., Hu, Y., Zhao, Y., Liu, H. and Zhou, D.-X. (2007). A *WUSCHEL*-LIKE *HOMEBOX* gene represses a *YABBY* gene expression required for rice leaf development. *Plant Physiol.* **144**, 380–390.
- Eklund, D. M., Ståldal, V., Valsecchi, I., Cierlik, I., Eriksson, C., Hiratsu, K., Ohme-Takagi, M., Sundström, J. F., Thelander, M., Ezcurra, I. et al. (2010). The *Arabidopsis thaliana* *STYLISH1* protein acts as a transcriptional activator regulating auxin biosynthesis. *Plant Cell* **22**, 349–363.
- Eklund, D. M., Cierlik, I., Ståldal, V., Claes, A. R., Vestman, D., Chandler, J. and Sundberg, E. (2011). Expression of *Arabidopsis* *SHORT INTERNODES/STYLISH* family genes in auxin biosynthesis zones of aerial organs is dependent on a GCC box-like regulatory element. *Plant Physiol.* **157**, 2069–2080.
- Endo, M., Mikami, M. and Toki, S. (2015). Multigene knockout utilizing off-target mutations of the CRISPR/Cas9 system in rice. *Plant Cell Physiol.* **56**, 41–47.
- Forestan, C., Meda, S. and Varotto, S. (2010). ZmPIN1-mediated auxin transport is related to cellular differentiation during maize embryogenesis and endosperm development. *Plant Physiol.* **152**, 1373–1390.
- Friml, J., Vieten, A., Sauer, M., Weijers, D., Schwarz, H., Hamann, T., Offringa, R. and Jürgens, G. (2003). Efflux-dependent auxin gradients establish the apical-basal axis of *Arabidopsis*. *Nature* **426**, 147–153.
- Giulini, A., Wang, J. and Jackson, D. (2004). Control of phyllotaxy by the cytokinin-inducible response regulator homologue *ABPHYL1*. *Nature* **430**, 1031–1034.
- Hibara, K. and Nagato, Y. (2005). *Petunia* *NO APICAL MERISTEM* ortholog, *OsNAM*, is expressed in the embryonic SAM and organ boundary in rice. *Rice Genet. Newsletter* **22**, 79–81.
- Hirano, K., Aya, K., Hobo, T., Sakakibara, H., Kojima, M., Shim, R. A., Hasegawa, Y., Ueguchi-Tanaka, M. and Matsuoka, M. (2008). Comprehensive transcriptome analysis of phytohormone biosynthesis and signaling genes in microspore/pollen and tapetum of rice. *Plant Cell Physiol.* **49**, 1429–1450.
- Hirose, N., Makita, N., Kojima, M., Kamada-Nobusada, T. and Sakakibara, H. (2007). Overexpression of a type-A response regulator alters rice morphology and cytokinin metabolism. *Plant Cell Physiol.* **48**, 523–539.
- Itoh, H., Shimada, A., Ueguchi-Tanaka, M., Kamiya, N., Hasegawa, Y., Ashikari, M. and Matsuoka, M. (2005a). Overexpression of a GRAS protein lacking the DELLA domain confers altered gibberellin responses in rice. *Plant J.* **44**, 669–679.
- Itoh, J., Nonomura, K., Ikeda, K., Yamaki, S., Inukai, Y., Yamagishi, H., Kitano, H. and Nagato, Y. (2005b). Rice plant development: from zygote to spikelet. *Plant Cell Physiol.* **46**, 23–47.
- Jenik, P. D., Gillmor, C. and Lukowitz, W. (2007). Embryonic Patterning in *Arabidopsis thaliana*. *Annu. Rev. Cell Dev. Biol.* **23**, 207–236.
- Jiao, Y., Tausta, S. L., Gandotra, N., Sun, N., Liu, T., Clay, N. K., Ceserani, T., Chen, M., Ma, L., Holford, M. et al. (2009). A transcriptome atlas of rice cell types uncovers cellular, functional and developmental hierarchies. *Nat. Genet.* **41**, 258–263.
- Kaneko, M., Itoh, H., Inukai, Y., Sakamoto, T., Ueguchi-Tanaka, M., Ashikari, M. and Matsuoka, M. (2003). Where do gibberellin biosynthesis and gibberellin signaling occur in rice plants? *Plant J.* **35**, 104–115.
- Lau, S., Slane, D., Herud, O., Kong, J. and Jürgens, G. (2012). Early embryogenesis in flowering plants: setting up the basic body pattern. *Annu. Rev. Plant Biol.* **63**, 483–506.
- Le, B. H., Cheng, C., Bui, A. Q., Wagmaster, J. A., Henry, K. F., Pelletier, J., Kwong, L., Belmonte, M., Kirkbride, R., Horvath, S. et al. (2010). Global analysis of gene activity during *Arabidopsis* seed development and identification of seed-specific transcription factors. *Proc. Natl. Acad. Sci. USA* **107**, 8063–8070.
- Le Hir, R. and Bellini, C. (2013). The plant-specific Dof transcription factors family: new players involved in vascular system development and functioning in *Arabidopsis*. *Front. Plant Sci.* **4**, 164.
- Lee, B.-H., Johnston, R., Yang, Y., Gallavotti, A., Kojima, M., Travençolo, B. A. N., Costa, L. d. F., Sakakibara, H. and Jackson, D. (2009). Studies of aberrant *phyllotaxy1* mutants of maize indicate complex interactions between auxin and cytokinin signaling in the shoot apical meristem. *Plant Physiol.* **150**, 205–216.
- Li, E., Wang, S., Liu, Y., Chen, J.-G. and Douglas, C. J. (2011). OVATE FAMILY PROTEIN4 (OFF4) interaction with KNAT7 regulates secondary cell wall formation in *Arabidopsis thaliana*. *Plant J.* **67**, 328–341.
- Liu, H.-L., Xu, Y.-Y., Xu, Z.-H. and Chong, K. (2007). A rice *YABBY* gene, *OsYABBY4*, preferentially expresses in developing vascular tissue. *Dev. Genes Evol.* **217**, 629–637.
- Lu, X., Chen, D., Shu, D., Zhang, Z., Wang, W., Klukas, C., Chen, L.-L., Fan, Y., Chen, M. and Zhang, C. (2013). The differential transcription network between embryo and endosperm in the early developing maize seed. *Plant Physiol.* **162**, 440–455.
- Möller, B. and Weijers, D. (2009). Auxin control of embryo patterning. *Cold Spring Harb. Perspect. Biol.* **1**, a001545.
- Müller, B. and Sheen, J. (2008). Cytokinin and auxin interaction in root stem-cell specification during early embryogenesis. *Nature* **453**, 1094–1097.
- Nagasawa, N., Hibara, K.-I., Heppard, E. P., Vander Velden, K. A., Luck, S., Beatty, M., Nagato, Y. and Sakai, H. (2013). *GIANT EMBRYO* encodes CYP78A13, required for proper size balance between embryo and endosperm in rice. *Plant J.* **75**, 592–605.
- Nakamura, A., Fujioka, S., Sunohara, H., Kamiya, N., Hong, Z., Inukai, Y., Miura, K., Takatsuto, S., Yoshida, S., Ueguchi-Tanaka, M. et al. (2006). The role of *OsBRL1* and its homologous genes, *OsBRL1* and *OsBRL3*, in rice. *Plant Physiol.* **140**, 580–590.
- Nardmann, J., Zimmermann, R., Durantini, D., Kranz, E. and Werr, W. (2007). *WOX* gene phylogeny in *Poaceae*: a comparative approach addressing leaf and embryo development. *Mol. Biol. Evol.* **24**, 2474–2484.
- Natesh, S. and Rau, M. A. (1984). *The Embryo; Embryology of Angiosperms*, pp. 377–443. Berlin, Heidelberg: Springer.
- Nordine, M. D. and Bartel, D. P. (2010). MicroRNAs prevent precocious gene expression and enable pattern formation during plant embryogenesis. *Genes Dev.* **24**, 2678–2692.
- Palovaara, J., Saiga, S. and Weijers, D. (2013). Transcriptomics approaches in the early *Arabidopsis* embryo. *Trends Plant Sci.* **18**, 514–521.

- Pérez-Rodríguez, P., Riaño-Pachón, D. M., Corrêa, L. G. G., Rensing, S. A., Kersten, B. and Mueller-Roeber, B. (2010). PlnTFDB: updated content and new features of the plant transcription factor database. *Nucleic Acids Res.* **38**, D822-D827.
- Rice Annotation Project (2008). The rice annotation project database (RAP-DB): 2008 update. *Nucleic Acids Res.* **36**, D1028-D1033.
- Sato, Y., Hong, S. K., Tagiri, A., Kitano, H., Yamamoto, N., Nagato, Y. and Matsuoka, M. (1996). A rice homeobox gene, *OSH1*, is expressed before organ differentiation in a specific region during early embryogenesis. *Proc. Natl. Acad. Sci. USA* **93**, 8117-8122.
- Sato, Y., Antonio, B. A., Namiki, N., Takehisa, H., Minami, H., Kamatsuki, K., Sugimoto, K., Shimizu, Y., Hirochika, H. and Nagamura, Y. (2011). RiceXPro: a platform for monitoring gene expression in japonica rice grown under natural field conditions. *Nucleic Acids Res.* **39**, D1141-D1148.
- Sato, Y., Takehisa, H., Kamatsuki, K., Minami, H., Namiki, N., Ikawa, H., Ohyanagi, H., Sugimoto, K., Antonio, B. A. and Nagamura, Y. (2013). RiceXPro version 3.0: expanding the informatics resource for rice transcriptome. *Nucleic Acids Res.* **41**, D1206-D1213.
- Sentoku, N., Sato, Y., Kurata, N., Ito, Y., Kitano, H. and Matsuoka, M. (1999). Regional expression of the rice KN1-type homeobox gene family during embryo, shoot, and flower development. *Plant Cell* **11**, 1651-1664.
- Shpak, E. D., Berthiaume, C. T., Hill, E. J. and Torii, K. U. (2004). Synergistic interaction of three ERECTA-family receptor-like kinases controls *Arabidopsis* organ growth and flower development by promoting cell proliferation. *Development* **131**, 1491-1501.
- Smith, D. L. and Fedoroff, N. V. (1995). *LRP1*, a gene expressed in lateral and adventitious root primordia of *Arabidopsis*. *Plant Cell* **7**, 735-745.
- Smith, Z. R. and Long, J. A. (2010). Control of *Arabidopsis* apical-basal embryo polarity by antagonistic transcription factors. *Nature* **464**, 423-426.
- Smyth, G. K. (2004). Linear models and empirical bayes methods for assessing differential expression in microarray experiments. *Stat. Appl. Genet. Mol. Biol.* **3**, 1-25.
- Spencer, M. W. B., Casson, S. A. and Lindsey, K. (2007). Transcriptional profiling of the *Arabidopsis* embryo. *Plant Physiol.* **143**, 924-940.
- Steeves, T. A. and Sussex, I. M. (1989). *Patterns in Plant Development*, 2nd edn. Cambridge, UK: Cambridge University Press.
- Takacs, E. M., Li, J., Du, C., Ponnala, L., Janick-Buckner, D., Yu, J., Muehlbauer, G. J., Schnable, P. S., Timmermans, M. C. P., Sun, Q. et al. (2012). Ontogeny of the maize shoot apical meristem. *Plant Cell* **24**, 3219-3234.
- Takahashi, H., Kamakura, H., Sato, Y., Shiono, K., Abiko, T., Tsutsumi, N., Nagamura, Y., Nishizawa, N. K. and Nakazono, M. (2010). A method for obtaining high quality RNA from paraffin sections of plant tissues by laser microdissection. *J. Plant. Res.* **123**, 807-813.
- Takehisa, H., Sato, Y., Igarashi, M., Abiko, T., Antonio, B. A., Kamatsuki, K., Minami, H., Namiki, N., Inukai, Y., Nakazono, M. et al. (2011). Genome-wide transcriptome dissection of the rice root system: implications for developmental and physiological functions. *Plant J.* **69**, 126-140.
- Toriba, T., Harada, K., Takamura, A., Nakamura, H., Ichikawa, H., Suzuki, T. and Hirano, H.-Y. (2007). Molecular characterization the YABBY gene family in *Oryza sativa* and expression analysis of *OsYABBY1*. *Mol. Genet. Genomics* **277**, 457-468.
- Ueda, M., Zhang, Z. and Laux, T. (2011). Transcriptional activation of *Arabidopsis* axis patterning genes *WOX8/9* links zygote polarity to embryo development. *Dev. Cell* **20**, 264-270.
- Wang, J.-R., Hu, H., Wang, G.-H., Li, J., Chen, J.-Y. and Wu, P. (2009). Expression of *PIN* genes in rice (*Oryza sativa* L.): tissue specificity and regulation by hormones. *Mol. Plant* **2**, 823-831.
- West, M. A. L. and Harada, J. J. (1993). Embryogenesis in higher plants: an overview. *Plant Cell* **5**, 1361-1369.
- Winter, D., Vinegar, B., Nahal, H., Ammar, R., Wilson, G. V. and Provart, N. J. (2007). An 'Electronic Fluorescent Pictograph' browser for exploring and analyzing large-scale biological data sets. *PLoS ONE* **2**, e718.
- Xu, H., Gao, Y. and Wang, J. (2012). Transcriptomic analysis of rice (*Oryza sativa*) developing embryos using the RNA-Seq technique. *PLoS ONE* **7**, e30646.
- Xue, L. J., Zhang, J. J. and Xue, H. W. (2011). Genome-wide analysis reveals gene expression and metabolic network dynamics during embryo development in *Arabidopsis*. *Plant Physiol.* **156**, 346-356.
- Xue, L.-J., Zhang, J.-J. and Xue, H.-W. (2012). Genome-wide analysis of the complex transcriptional networks of rice developing seeds. *PLoS ONE* **7**, e31081.
- Zhou, S.-R., Yin, L.-L. and Xue, H.-W. (2013). Functional genomics based understanding of rice endosperm development. *Curr. Opin. Plant Biol.* **16**, 236-246.

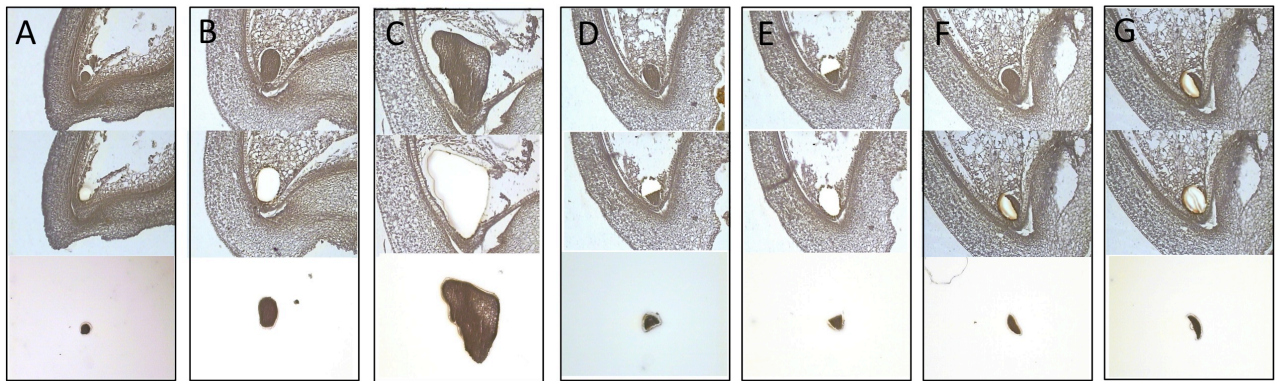


Figure S1. Laser microdissection of early embryo.

(A) Whole embryo at 2 DAP. (B) Whole embryo at 3 DAP. (C) Whole embryo at 4 DAP. (D) Apical half of the embryo at 3 DAP. (E) Basal half of the embryo at 3 DAP. (F) Ventral half of the embryo at 3 DAP. (G) Dorsal half of the embryo at 3 DAP. Top, middle and bottom are images of before dissection, after dissection, and a collected sample, respectively.

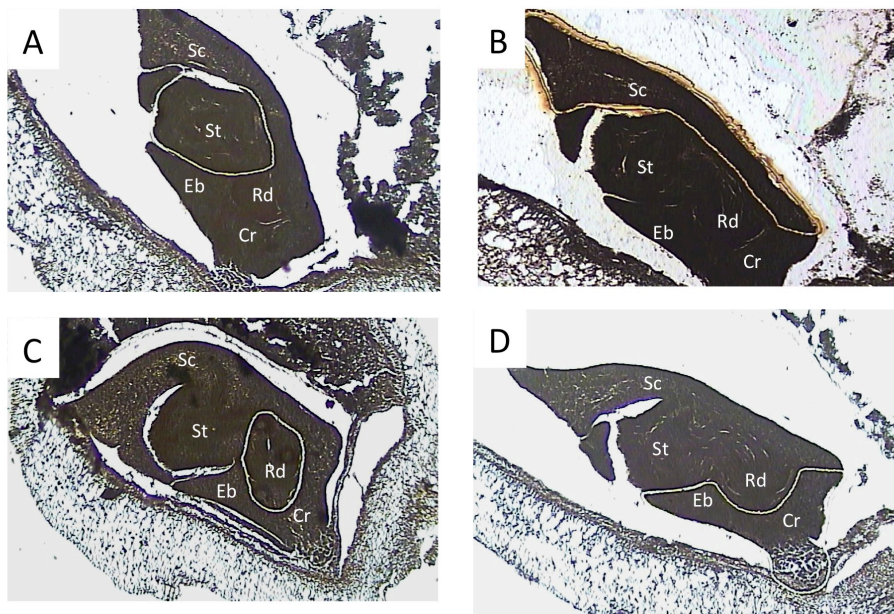


Figure S2. Laser microdissection of 7-DAP embryo.

(A) Separation of shoot containing tissue. (B) Scutellum. (C) Radicle (Root). (D) Epiblast/coleorhizae.
Ct: coleoptile, Sc: scutellum, Rd: radicle, St: shoot, Eb: epiblast, Cr: coleorhiza

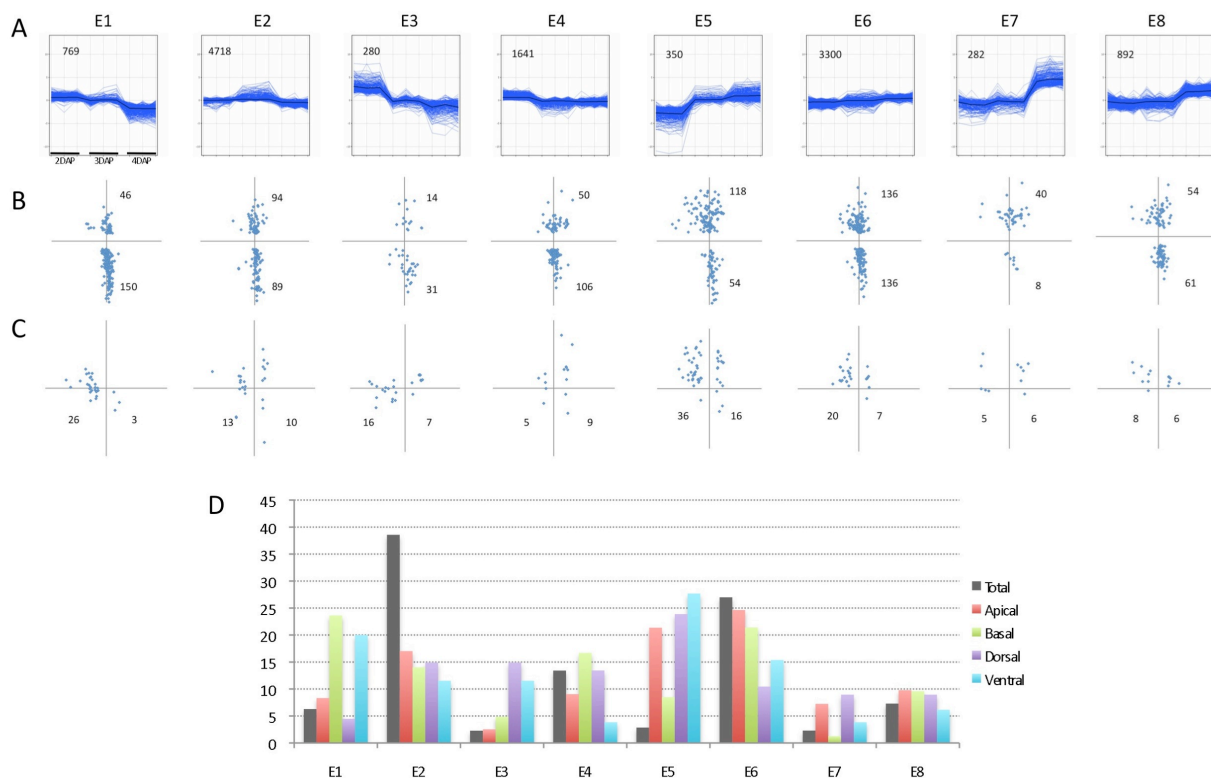


Figure S3. K-means clustering of gene expression in 3-DAP embryos.

(A) Changes in the expression levels of genes in the eight clusters. The X-axis represents 2-, 3-, and 4-DAP samples in triplicate. Y-axis represents the relative expression value of each probe. The number of probes categorized in the cluster is indicated in the upper left. (B) Expression sites of genes significantly biased along the apical-basal axis of 3-DAP embryos in each cluster. X- and Y-axes indicate the relative expression values (\log_2) along the dorsal-ventral and apical-basal axes, respectively. Numbers of genes preferentially expressed in the apical and basal regions are indicated. (C) Expression sites of genes significantly biased along the dorsal-ventral axis of 3-DAP embryos in each cluster. Numbers of genes preferentially expressed in the dorsal and ventral regions are indicated. (D) Percentages of genes contained in each cluster and region. Gray bar indicates the percentage of clustered genes compared to the total number of expressed genes. Red, green, purple and blue bars indicate the percentage of preferentially expressed genes in the apical, basal, dorsal and ventral regions compared to the total number of genes expressed in those regions.

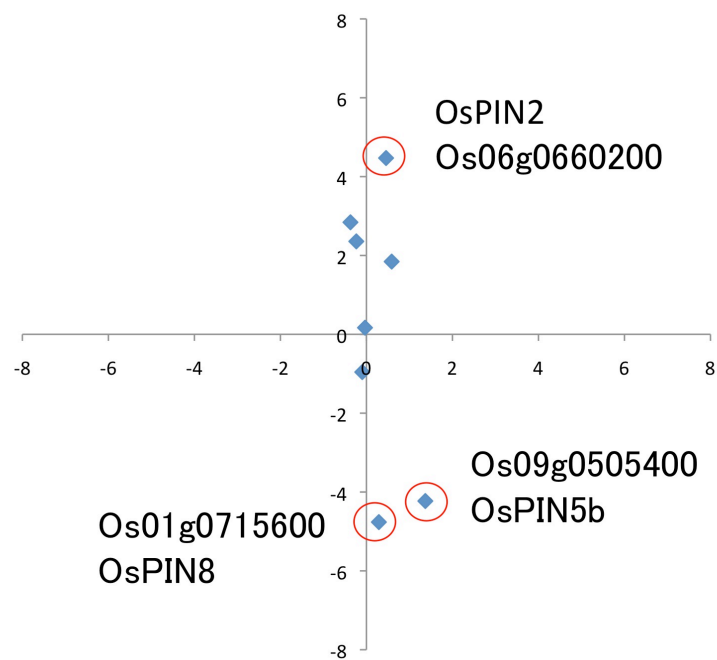


Figure S4. Spatial distribution of PIN-like genes in 3-DAP embryo.

Expression sites of PIN-like genes expressed in the 3DAP embryo in the scatter diagram. X- and Y-axis indicate the relative expression values (log2) along the dorsal-ventral and the apical-basal axis, respectively. Red circles indicate probes that showed conspicuously biased expression along the dorsal-ventral and/or the apical-basal axis as outliers. The RAP-ID and the annotation of the outliers are represented.

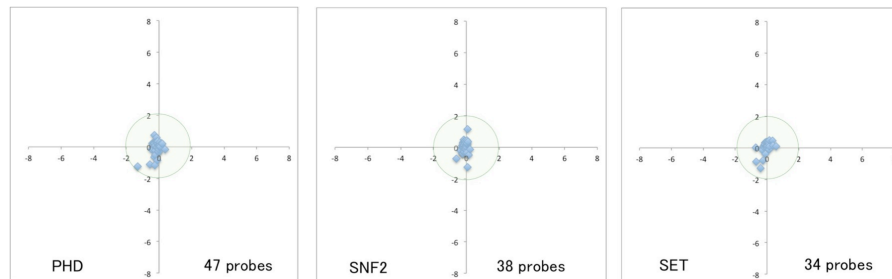


Figure S5. Spatial distribution of transcriptional factor and transcriptional regulator genes categorized into Type III.

Sites of transcription factor (TF) and transcriptional regulator (TR) genes expression in 3-DAP embryos in the scatter diagram. X- and Y-axes indicate the relative expression values (log2) along the dorsal-ventral and apical-basal axes, respectively. Data points inside the green circle represent probes with absolute relative expression values of less than 2.

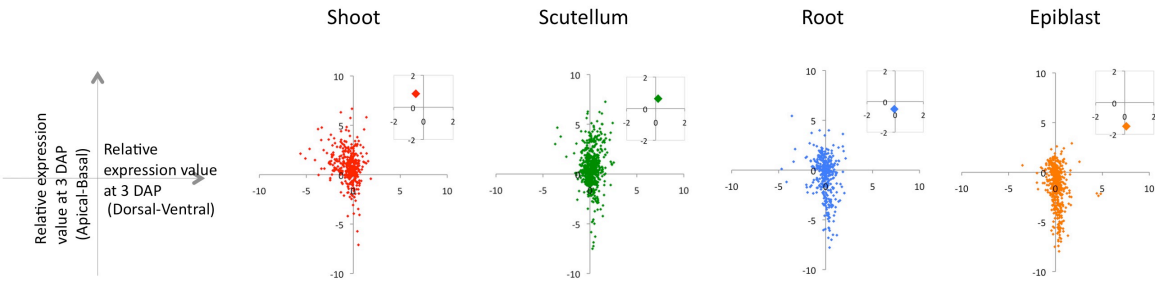


Figure S6. Spatial correlation between expression profiles in globular embryo and in embryonic organs at the later stage. Spatial expression pattern of genes upregulated in specific tissues of 7DAP embryos at 3DAP. Titles of the X- and Y-axes are presented in the leftmost diagram. Insets indicate the barycenters of the data points. Red, green, blue, and orange points represent the shoot, scutellum, root, and epiblast samples, respectively, of 7-DAP embryos.

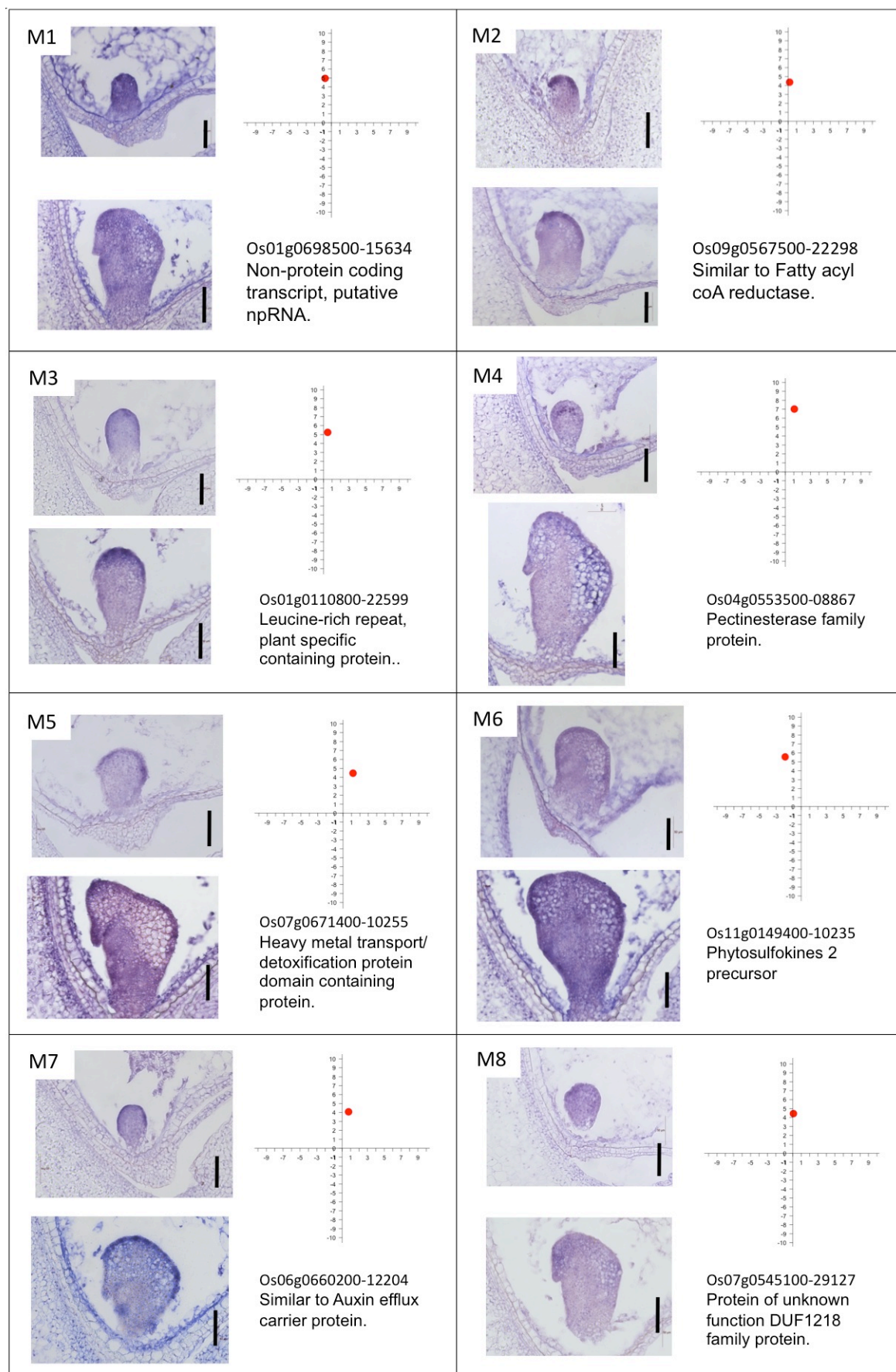


Figure S7. *In situ* expression pattern of the selected genes that are not included in the Figure 5.

On the left of the upper and lower images of each panel are the expression patterns of 3- and 4-DAP embryos, respectively. The right scatter diagram indicates the predicted expression site of the corresponding probe based on microarray analysis. The RAP-ID, probe number, annotations and marker ID (see supplementary material Table S10) of the genes are indicated. Scale bars = 50 μ m.

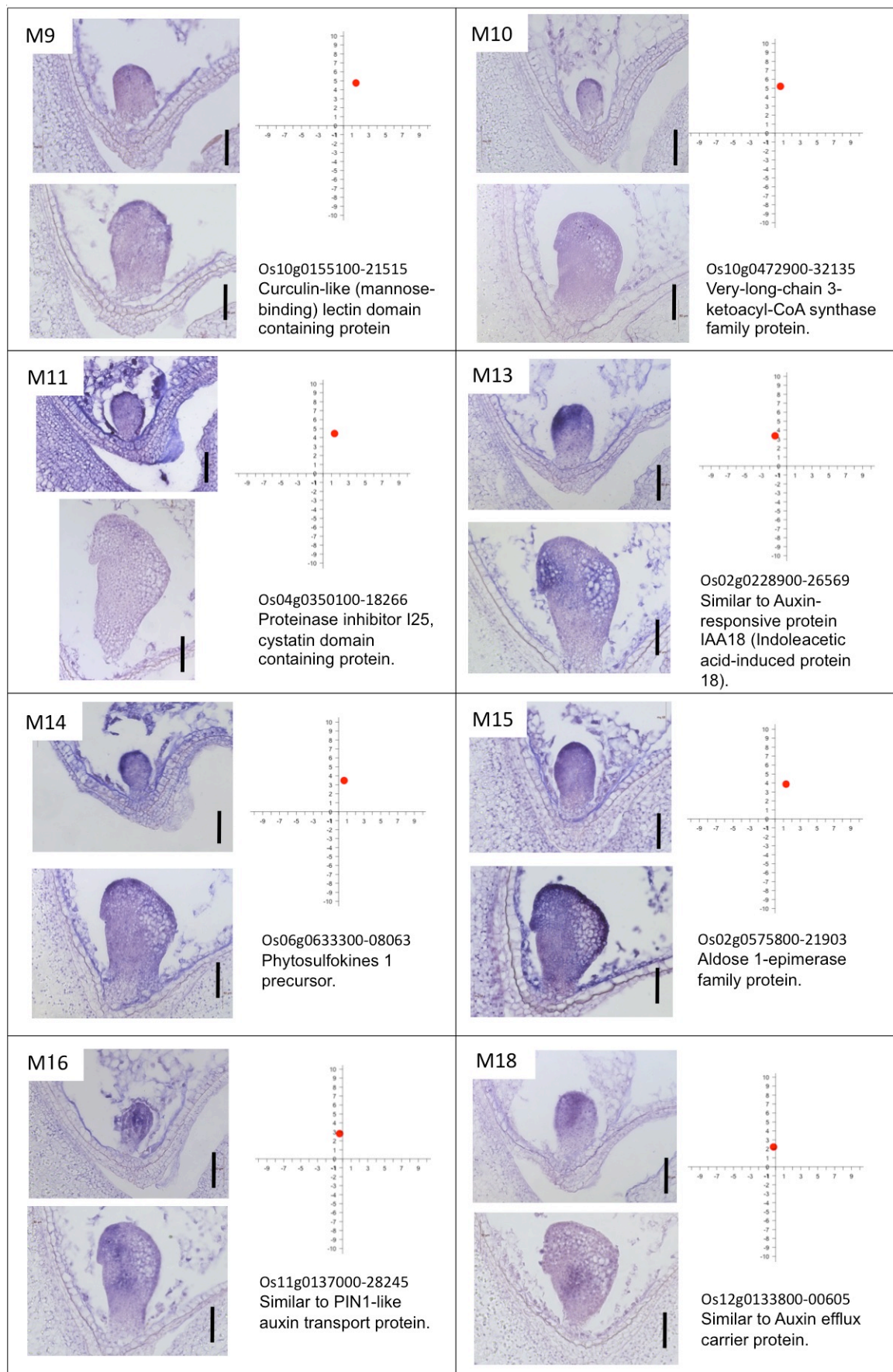


Figure S7. Cont'd.

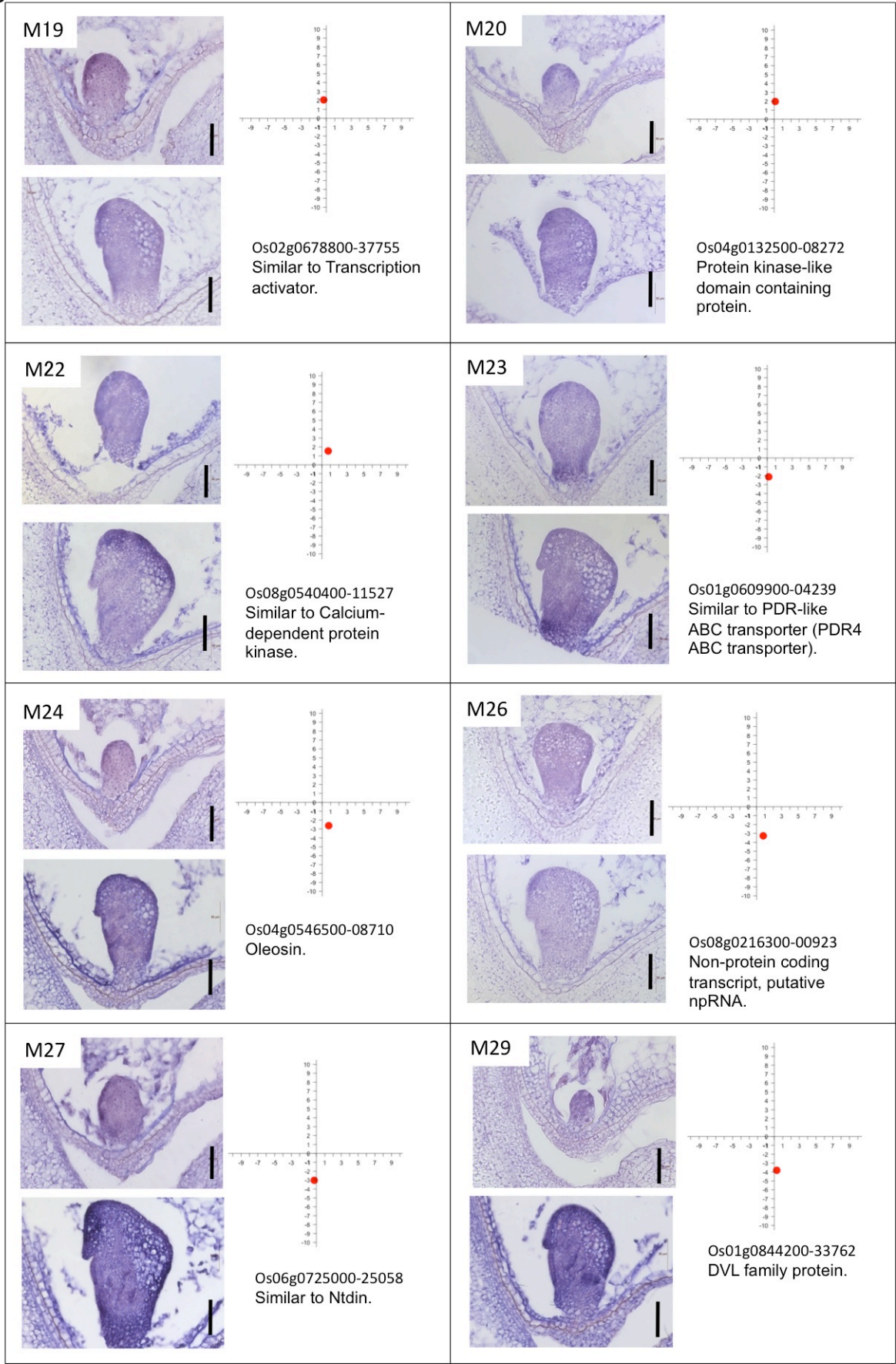


Figure S7. Cont'd.

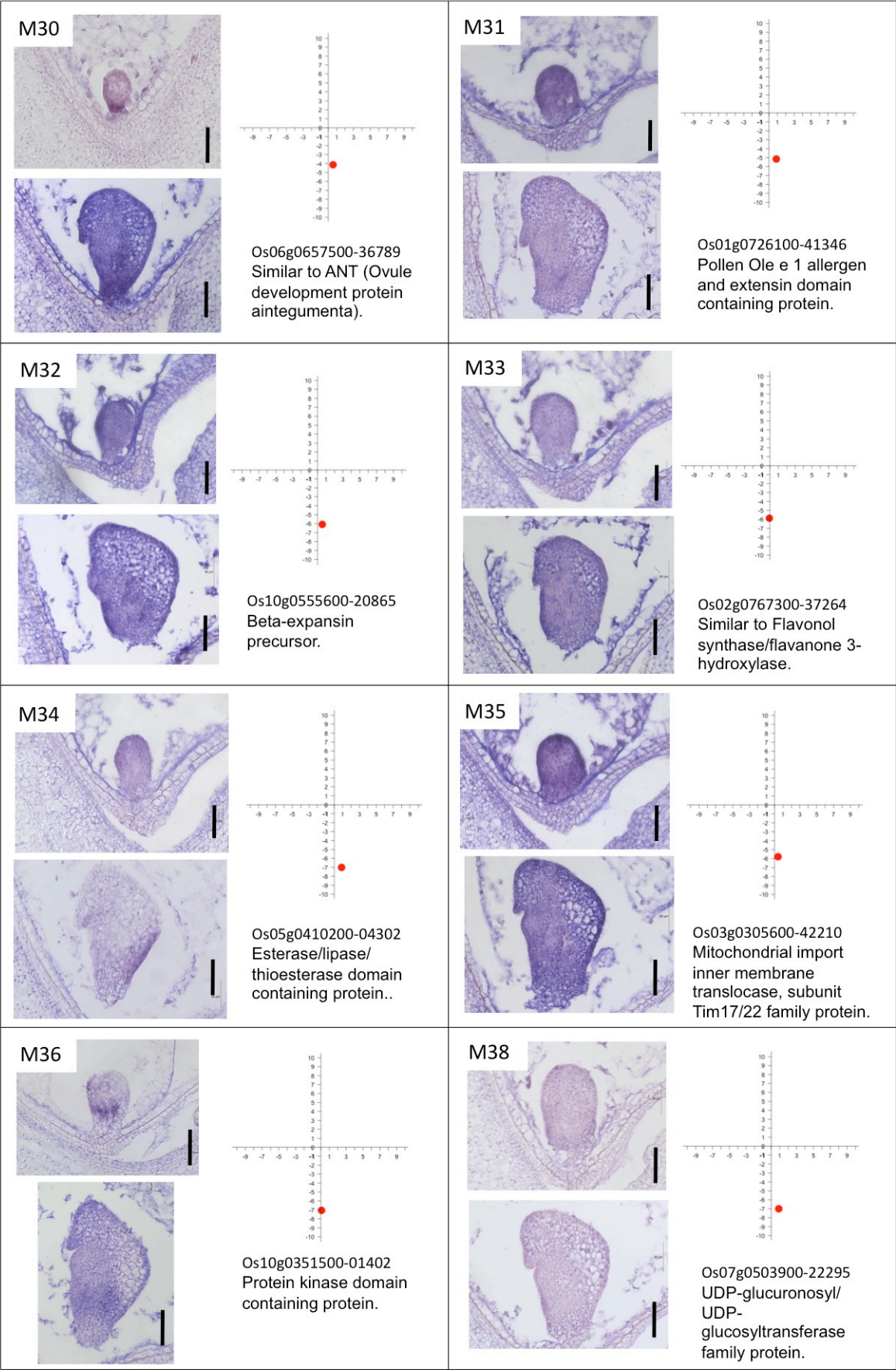


Figure S7. Cont'd.

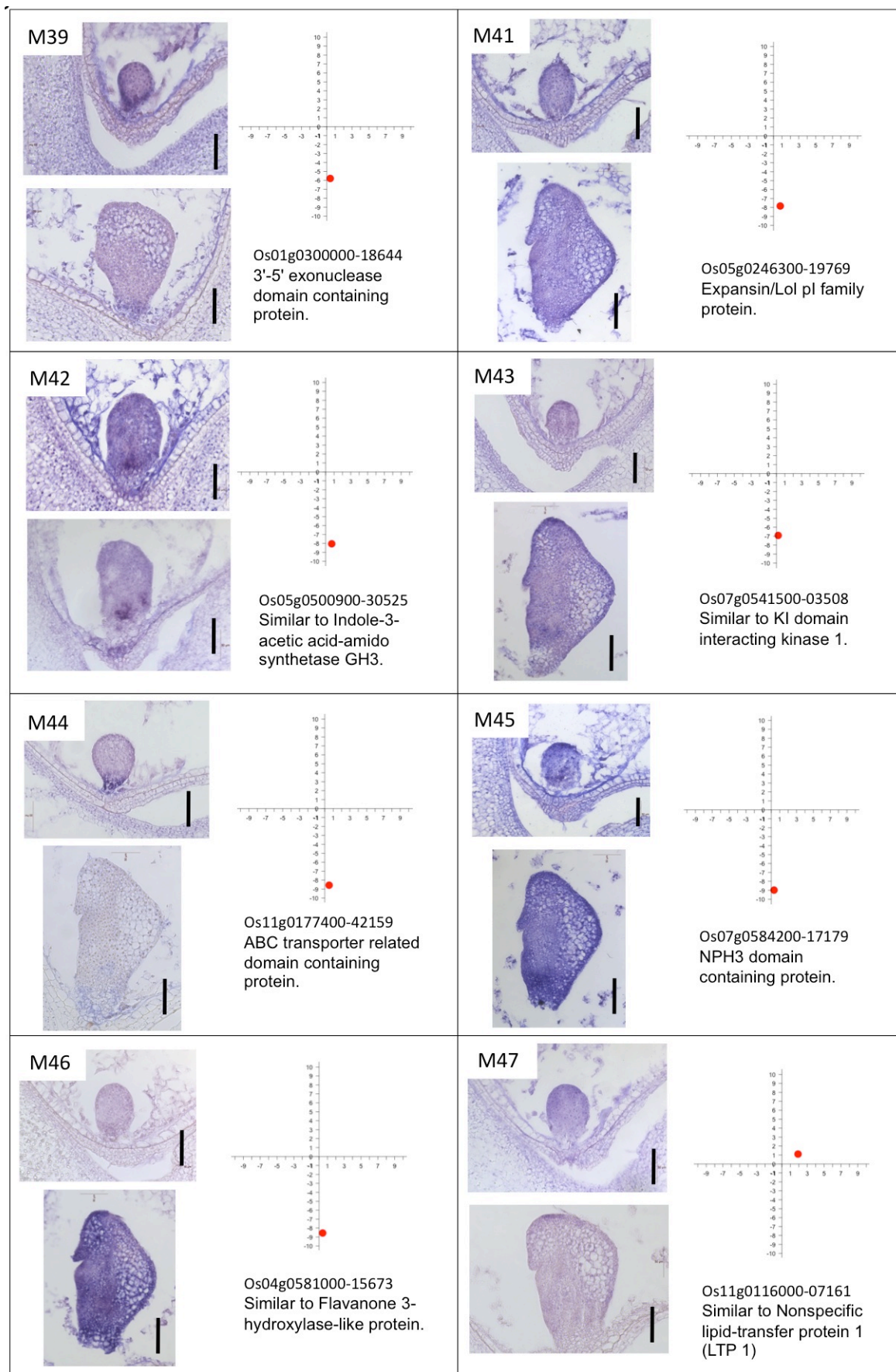


Figure S7. Cont'd.

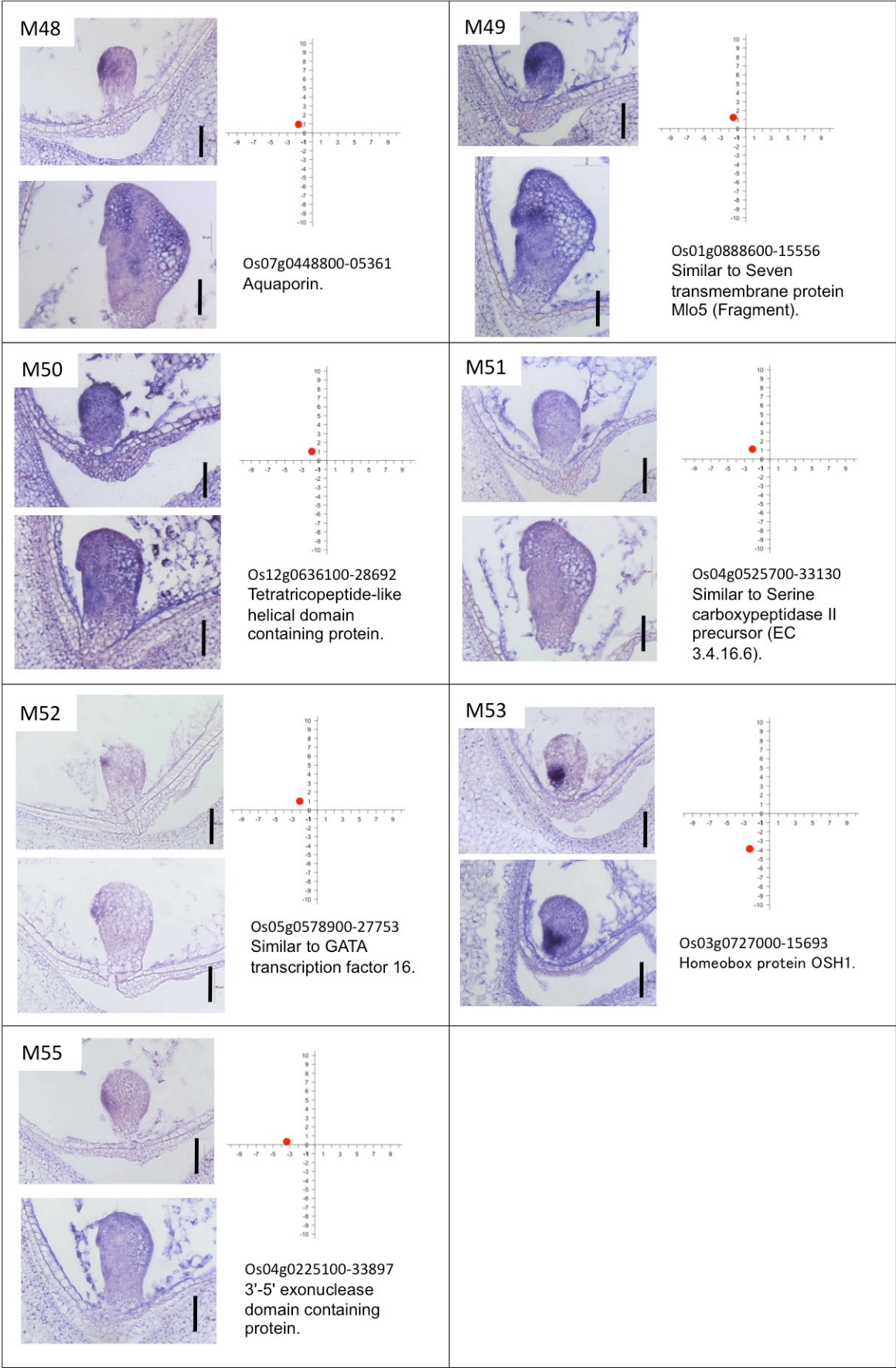


Figure S7. Cont'd.

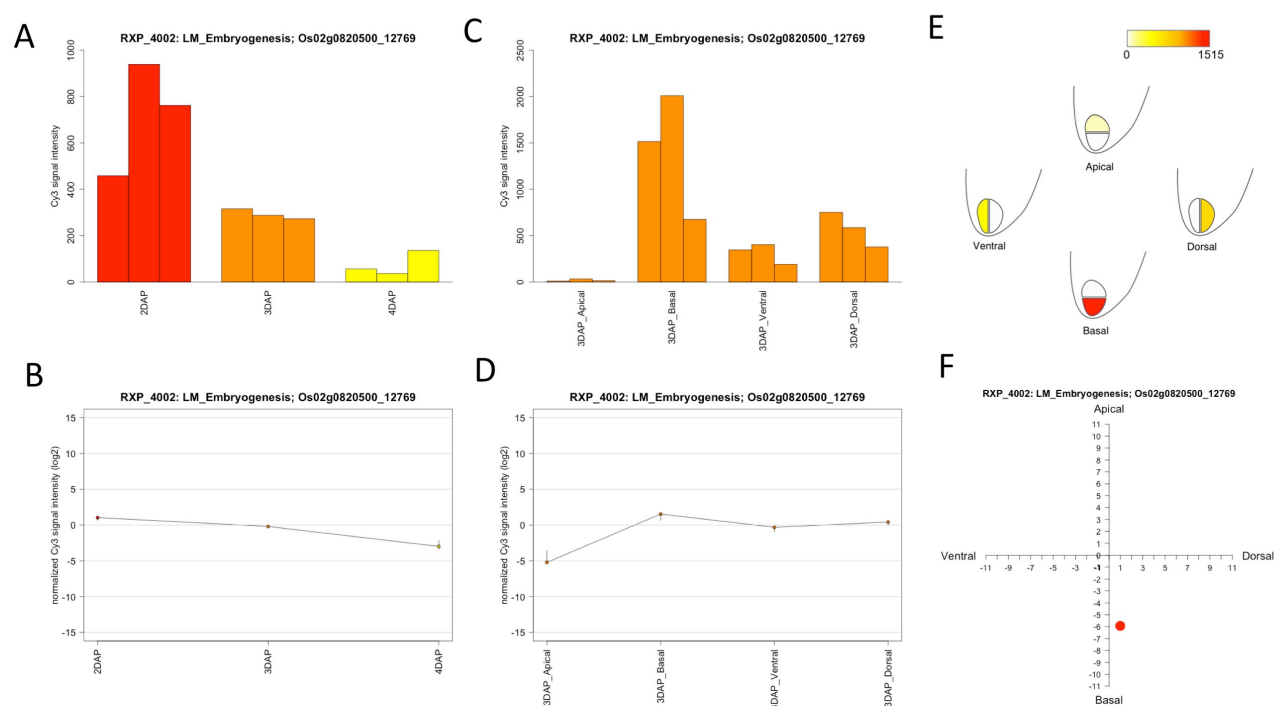


Figure S8. Gene expression profiles during early embryogenesis, as shown in the RiceXPro database. Schematic of the expression pattern of Os02g0820500 in the ‘temporal’ and ‘spatial’ data sets. (A) Raw signal intensity of whole embryos at 2, 3 and 4 DAP. Three replicates are shown. (B) Normalized signal intensity of whole embryos at 2, 3 and 4 DAP. (C) Raw signal intensity of the apical, basal, ventral and dorsal embryonic regions at 3 DAP. (D) Normalized signal intensity of the four embryonic regions at 3 DAP. (E) Pictograph of expression intensity among the four embryonic regions. (F) Scatter diagram of expression sites in 3-DAP embryos.

Table S1. Pearson correlation coefficient among the entire set of normalized data.

[Click here to Download Table S1](#)

Table S2. The list of the genes that are preferentially expressed in the apical and basal region of 3-DAP embryo.

[Click here to Download Table S2](#)

Table S3. The list of the genes that are preferentially expressed in the dorsal and ventral region of 3-DAP embryo.

[Click here to Download Table S3](#)

Table S4. The list of the genes that are preferentially expressed in the apical-dorsal, apical-ventral, basal-dorsal and basal-ventral regions of 3-DAP embryo.

[Click here to Download Table S4](#)

Table S5. The list of the genes that are categorized by K-means clustering of 3-DAP embryo.

[Click here to Download Table S5](#)

Table S6. The list of the genes that are preferentially expressed in the apical, basal, dorsal and ventral region in each cluster.

[Click here to Download Table S6](#)

Table S7. The list of the genes and their expression profiles of phytohormone-related genes in 3-DAP embryo.

[Click here to Download Table S7](#)

Table S8. The list of the genes and their expression profiles of transcriptional factor and transcriptional regulator genes in 3-DAP embryo.

[Click here to Download Table S8](#)

Table S9. The list of the genes that are preferentially expressed in the shoot, epiblast, scutellum and root containing tissues of 7-DAP embryos.

[Click here to Download Table S9](#)

Table S10. The list of the selected genes as markers of *in situ* hybridization for early embryogenesis.

[Click here to Download Table S10](#)